

MAGNETISM and MAGNETIC MATERIALS

Magnetization Characteristics of Conductive Ferrites

Aldissi, M., Fractal Systems, Inc.
Hall, D., NHMFL

Magnetization measurements were performed on powders of the MnZn ferrite particulates (10 to 15 μm average diameter) and the ferrite coated with 1.5 and 3.0 weight % nickel (see Fig. 1) at the NHMFL in Tallahassee. The symmetrical shape is expected from such soft ferromagnets. The main goal of this type of measurement for these three samples was to find out the effect of nickel coating at the particle level on the overall magnetic properties of the ferrite. The results have shown that, although electrical conductivity (bulk property) has increased upon coating the ferrite particles with a thin layer of nickel,

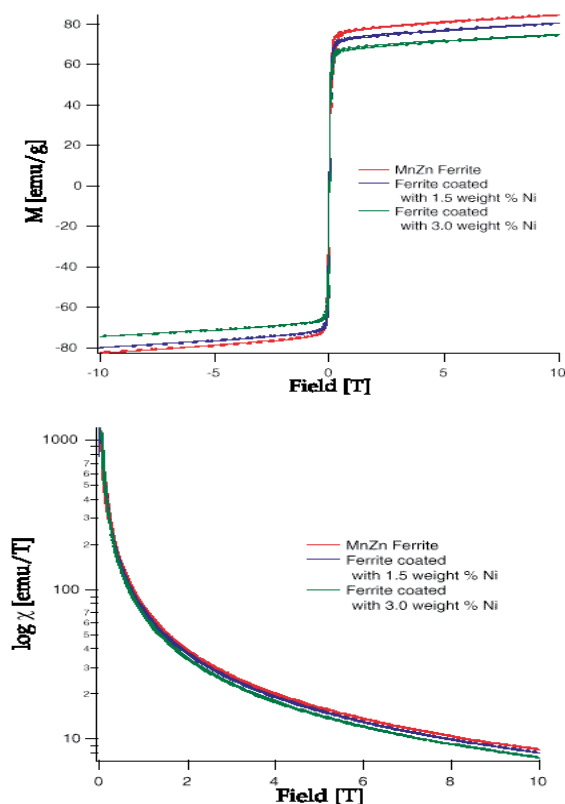


Figure 1. Magnetization curves of ferrite and nickel-coated ferrite.

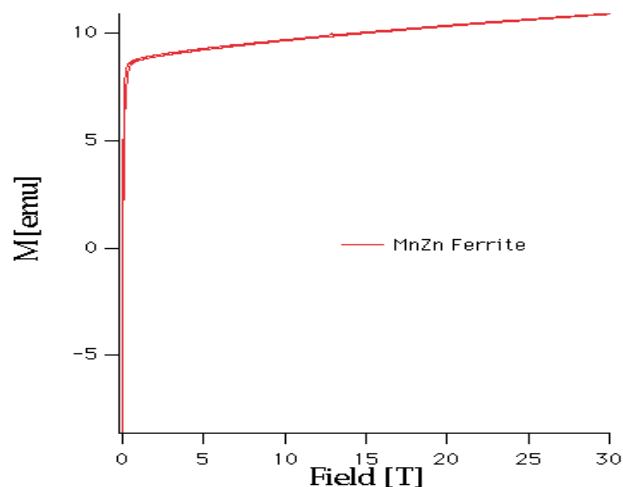


Figure 2. Magnetization curves of ferrite up to 30 T.

their magnetic properties are practically unchanged. This type of measurement proved feasibility of making soft ferromagnets with higher electrical conductivity and without the penalty of diluting their magnetic properties. Fig. 2 shows the magnetization data for the ferrite powder up to 30 T with no unexpected transition in the magnetization curve. Magnetization is enhanced as the field becomes stronger, which is again a property of soft ferromagnets.

Acknowledgements: This research was sponsored by the Ballistic Missile Defense Organization (BMDO/IST), and managed by the U.S. Army Space and Missile Defense Command.

Observation of Shubnikov – deHaas Oscillations in BaRuO_3

Alexander, C.S., NHMFL
Zhou, Z.X., NHMFL
Balicas, L., NHMFL
McCall, S., NHMFL
Cao, G., NHMFL
Brooks, J.S., NHMFL
Crow, J.E., NHMFL

BaRuO_3 is a quasi one-dimensional metal that displays unusual and highly anisotropic transport behavior. In this material, Ru is +4 valent leaving four 4-d electrons in the outer shell, which, due to

large crystalline electric field splitting, are in the low ($S=1$) spin state. Due to the broader spatial extent of 4-d electrons, as compared to their 3-d counterparts, materials such as this provide an opportunity to explore for new phenomena. Here we briefly report the results of magnetotransport studies carried out at low temperature (30 mK) and high magnetic field (18 T) on high quality single crystals of the nine layer crystallographic form. The crystals have a rhombohedral close-packed structure with sets of three face-sharing RuO_6 octahedra along the c axis joined by corner sharing in the ab plane. These experiments were conducted using the Oxford Instruments 18 T superconducting magnet and a dilution-refrigerated cryostat in the DC High Field Facility in Tallahassee.

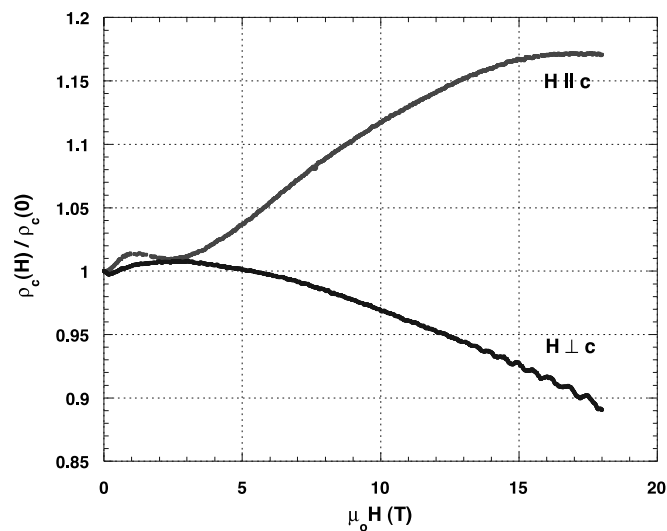


Figure 1. Magnetoresistance of BaRuO_3 with field applied parallel and perpendicular to the c axis.

Shown in Fig. 1 is the c axis magnetoresistance taken with the applied field both parallel and perpendicular to the c axis at 30 mK. Immediately obvious is the large anisotropy between the two measurements. For field applied parallel to the c axis, past a small and as yet unexplained peak, the sample shows increasingly positive magnetoresistance. This positive magnetoresistance is systematically reduced as the crystal is rotated reaching a minimum when the field is applied perpendicular to the c axis, in which case the magnetoresistance is negative. These results characterize the quasi one-dimensional behavior resultant from the crystal structure.

Oscillations can be seen in the magnetoresistance when the applied field is within 40 degrees of being perpendicular to the c axis. In the case of applied field perpendicular to the c axis, these oscillations are shown in the inset to Fig. 2. Upon Fourier analysis, a fundamental frequency of 400 T was detected in the oscillations as shown in the Fourier spectrum of Fig. 2. This single, relatively low frequency indicates that the observed oscillations are derived from a single small branch of the Fermi surface. Further study of this material at higher magnetic field is clearly indicated to gain a more complete picture of the Fermi surface.

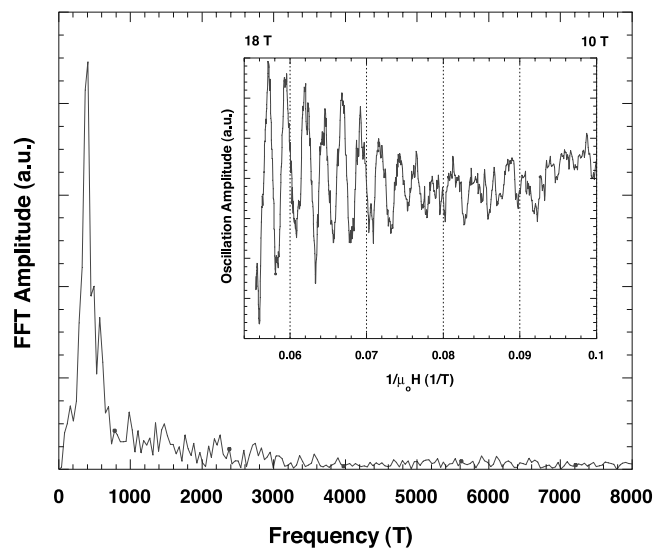


Figure 2. Fourier spectrum of Shubnikov - deHaas oscillations in BaRuO_3 . The magnetoresistance oscillation amplitude is shown in the inset.

Quantum Error-Correction and Topological Quantum Numbers

Bonesteel, N.E., NHMFL/FSU, Physics

One of the most surprising recent developments in quantum information theory has been the discovery of a scheme for fighting decoherence using what are called quantum error-correcting codes.¹ A quantum error-correcting code is a mapping from the Hilbert space of a single qubit to a subspace of the Hilbert space of many physical qubits. The resulting many qubit state is then referred to as an encoded qubit. These encoded states are carefully designed so that if

an error occurs, i.e., if a small number of the physical qubits become entangled with their environment, certain measurements can be performed to determine which error has occurred, and how it can be corrected without disturbing the quantum information stored in the encoded qubit.

Kitaev² has constructed quantum error-correcting codes using the degenerate ground states of a particular class of spin Hamiltonians realized on finite two-dimensional lattices with periodic boundary conditions. The degenerate ground states of these Hamiltonians are distinguished by topological quantum numbers which can only be determined by global measurements. Local measurements can therefore be performed on a given encoded state in order to determine whether and where an error has occurred without disturbing the encoded quantum information in that state.

Motivated by this connection between topological degeneracy and quantum error-correcting codes, the possibility of using the two-fold topological degeneracy of the spin-1/2 chiral spin liquid states on the torus³ to construct quantum error-correcting codes was investigated.⁴ It was shown that, unlike Kitaev's codes, codes constructed using chiral spin liquid states on finite periodic lattices do not meet the necessary and sufficient conditions for correcting even a single qubit error with perfect fidelity. However, for large enough lattice sizes, these conditions are approximately satisfied, and the resulting codes may be viewed as approximate quantum error correcting codes.

Acknowledgements: This work was supported by the U.S. Department of Energy under Grant No. DE-FG02-97ER45639.

¹ Shor, P.W., Phys. Rev. A, **52**, 2493 (1995).

² Kitaev, A.Y., quant-ph/9707021.

³ Wen, X.G., Phys. Rev. B, **40**, 7387 (1989).

⁴ Bonesteel, N.E., Phys. Rev. A, **62**, 62310 (2000).

⁷Li NMR Studies of the Spin Ladder Compound, LiCu₂O₂

Caldwell, T., NHMFL

Moulton, W.G., NHMFL/FSU, Physics

Reyes, A.P., NHMFL

Kuhns, P.L., NHMFL

Cao, G., NHMFL

Xin, Y., NHMFL

Crow, J.E., NHMFL

LiCu₂O₂ is a relatively new compound that contains both Cu⁺ and Cu²⁺ (magnetic) and has unusual magnetic properties. There has been some controversy over whether the structure is tetragonal or orthorhombic. It has now been well established (see Xin elsewhere in this publication) that the structure is tetragonal, and the Cu²⁺ form a two leg spin ladder. However, there is a small amount of a second phase, LiCuO present. Magnetization data show a large anisotropy, a broad, possibly antiferromagnetic, transition at about 25 K, and a second very sharp transition at 9 K only along the c axis. Both of these transitions are observed in the specific heat data. We have very recently carried out ⁷Li NMR experiments on a single crystal exhibiting these properties.

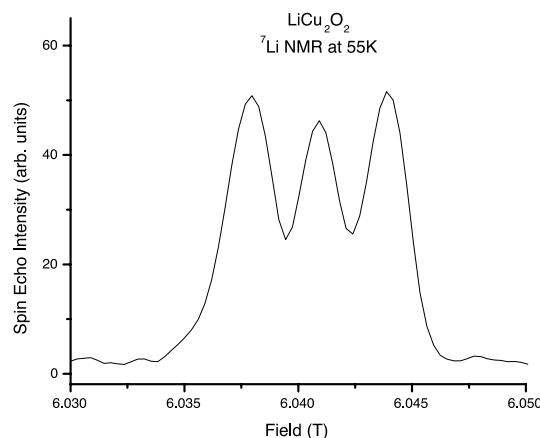


Figure 1. ⁷Li NMR spectrum at 55 K, 6 T (100 MHz) with B along the c axis.

As shown in Fig. 1, the spectrum at 55 K, well above the transition, with B along the c axis, shows a clearly resolved three line spectrum that collapses to a single line with B perpendicular to the c axis. In contrast to the one previous NMR¹ work on

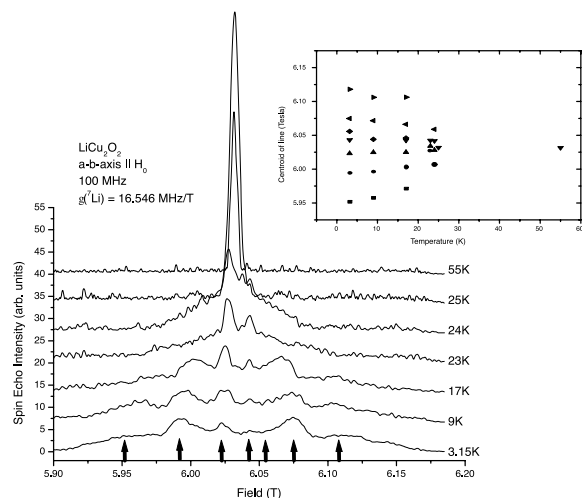


Figure 2. Temperature dependence of the spectrum for conditions of Fig. 1 below T_N .

LiCu_2O_2 powder samples, we attribute the spectrum to a highly anisotropic magnetic shift of three single unresolved quadrupolar lines due to the four different Li sites in the unit cell, rather than to quadrupole splitting as suggested earlier.¹ This interpretation is based on the field dependence of the splitting. The three lines rather than four, we attribute to the fact that two of the non-equivalent Li have qualitatively the same bond lengths and symmetry.

Calculation of the electric field gradients from a point charge model give electric field gradient variations at the different sites by a factor of four, roughly 10 to 40 KHz, and we thus believe the Zeeman splitting of the quadrupole coupling is buried within the linewidth. Below the transition at 25 K, with the field perpendicular to c , the spectrum splits into seven lines as shown in Fig. 2, which indicates a strong orientation dependence. This clearly shows that antiferromagnetic ordering occurs at 25 K, with a non-zero order parameter. For reasons not presently understood there is no obvious change in the spectrum below the 9 K transition. Further analysis of the data to quantitatively determine the temperature dependence of the magnetic shift and the spin configuration from the data below 25 K are in progress. Also, T_1 measurements in progress will be important to study the low frequency spin fluctuations above T_N .

¹ Fritschij, F.C., *et al.*, Sol. State. Comm., **107**, 719 (1998).

Diamagnetism in Magnetic Insulator $\text{Sr}_3\text{Ir}_2\text{O}_7$

Cao, G., NHMFL

Xin, Y., NHMFL

Alexander, C.S., NHMFL

Crow, J.E., NHMFL

Double layered $\text{Sr}_3\text{Ir}_2\text{O}_7$ single crystals were newly synthesized. The compound at room temperature crystallizes in a tetragonal unit cell ($a=3.896$ Å and $c=20.879$ Å) with space group $I4/mmm$. The IrO_6 octahedra are rotated about the c -axis by about 12° . As expected in most 4d- and 5d-electron compounds, Ir^{4+} ion ($5d^5$) in $\text{Sr}_3\text{Ir}_2\text{O}_7$ is in a low spin configuration t_{2g}^5 with $S=1/2$.

We have investigated structural (TEM, EDX and x-ray diffraction), transport and magnetic properties of this system. The results show that $\text{Sr}_3\text{Ir}_2\text{O}_7$ is a magnetic insulator with a weak ferromagnetic transition at $T_C=287$ K and a complex magnetic structure at lower temperatures. While data reveals interesting and unusual conducting behavior including anomalies at corresponding magnetic ordering temperatures that are insensitive to magnetic field, the most novel and peculiar phenomenon in $\text{Sr}_3\text{Ir}_2\text{O}_7$ is a diamagnetic response under *field-cooled* (FC) conditions shown in Fig. 1 where magnetization as a function of temperature is plotted. It is clear that the magnetization for the ab -plane measured using FC sequences shows an abrupt ferromagnetic-like transition at 287 K which is then followed by an anomalous downturn below 40 K characterized by a robust magnetization reversal. In contrast, no anomaly is discerned in the entire measured temperature range under zero-field-cooled (ZFC) conditions. This diamagnetic state becomes weaker as magnetic field increases and eventually vanishes at 5000 Oe.

A similar phenomenon, though with distinct features, has recently been observed in LaVO_3 and YVO_3 .^{1,2} It has been suggested that the diamagnetic response is a result of a reversal of a canted-spin moment due to the first-order Jahn-Teller phase transition below which the orbital angular momentum is maximized.

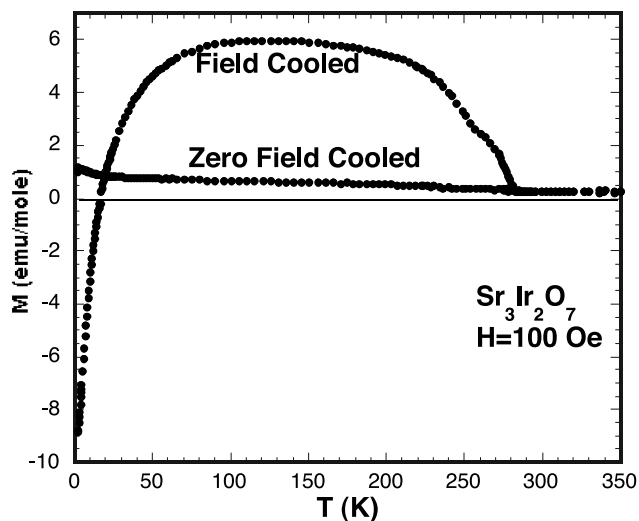


Figure 1. Magnetization vs. temperature for the ab-plane.

While the mechanism of the diamagnetic state in $\text{Sr}_3\text{Ir}_2\text{O}_7$ is yet to be understood, the phenomenon is evidently a consequence of a strong spin-orbit coupling that reverses the entire magnetic moment in opposition to the applied magnetic field. There are two possible mechanisms that may result in weak ferromagnetism or canted antiferromagnetism, namely, single ion anisotropy and antisymmetric Dzyaloshinsky-Moriya (DM) interactions. The DM superexchange, $\mathbf{D} \cdot (\mathbf{S}_1 \times \mathbf{S}_2)$ (where \mathbf{D} is the Dzyaloshinsky vector), is in competition with the ordinary Heisenberg exchange $\mathbf{J} \mathbf{S}_1 \cdot \mathbf{S}_2$, which prefers collinear spin configurations. The single ion anisotropy, which is due to the crystal electric field, creates a local easy axis that staggers the magnetic spins, thus weak ferromagnetism.

The observed diamagnetic state in $\text{Sr}_3\text{Ir}_2\text{O}_7$ could be attributed to a subtle competition between the two mechanisms. It is plausible that the weak ferromagnetic behavior at high temperatures is due to a large local magnetic anisotropy. As temperature decreases (below 40 K), the antisymmetric DM exchange motivated by a possible structural phase transition develops, and tends to cant the spins in the opposite direction. Accordingly, the net moment drops, cross zero and eventually becomes opposite to the magnetic field at temperatures (below 40 K for $H=100$ Oe) where the DM coupling dominates. The title material along with its sister compound Sr_2IrO_4 , which is a ferromagnet with $T_C=240$ K,

certainly merits further investigations in connection with our on-going research effort in exploring and understanding novel properties of 4d- and 5d transition metal oxides.

¹ Nyuyen, H.C., *et al.*, Phys. Rev. B, **52**, 324 (1995).

² Ren, Y., *et al.*, Nature, **396**, 441 (1998).

High Field Magnetotransport of Single-Crystal TmSb

Christianson, A.D., NHMFL/LANL

Lacerda, A.H., NHMFL/LANL

Touton, S., Occidental College, Physics

Fisher, I.R., Ames Laboratory and Iowa State Univ., Physics and Astronomy

Bud'ko, S.L., Ames Laboratory and Iowa State Univ., Physics and Astronomy

Canfield, P.C., Ames Laboratory and Iowa State Univ., Physics and Astronomy

Kern, S., Colorado State Univ., Physics

The origin of the transport properties of rare earth mononictides can be complicated due to the competition between several effects, such as crystal-field and magnetic exchange effects. TmSb is particularly attractive as it is thought to be a crystal-field only system. We have performed magnetotransport measurements on high quality single-crystals of TmSb. We find a residual

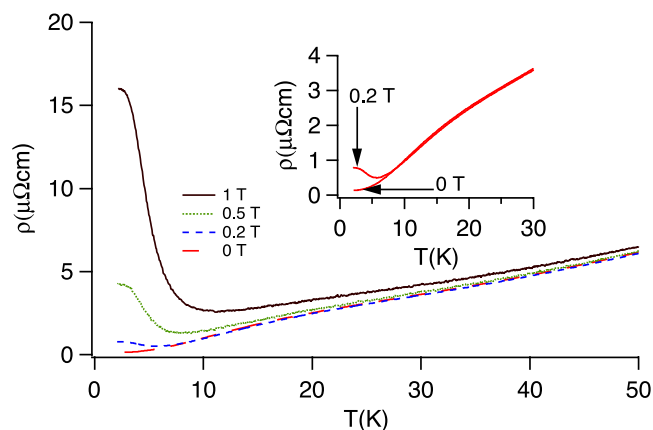


Figure 1. Low field magnetotransport. A broad maximum appears in the zero field transport. The inset shows the drastic change in low temperature behavior that occurs when a magnetic field of 0.2 T is applied.

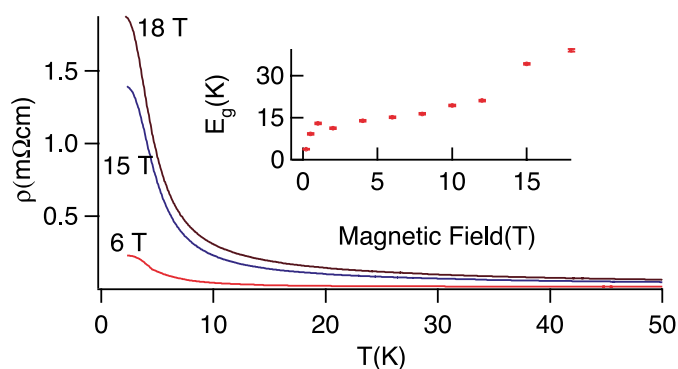


Figure 2. High field magnetotransport. Application of higher magnetic fields reveal qualitatively similar behavior to the low field case. In the inset, we have extracted an energy gap using activated dynamics.

resistivity ratio (RRR) of ~ 360 . Samples measured previously have RRRs at least an order of magnitude less. A broad feature is observed at 20 K in the zero field resistance, possibly due to crystal-field effects. Upon application of a magnetic field, this feature becomes smaller and is barely noticeable by 1 T. At low temperature the resistivity in applied magnetic fields behaves as if a pseudo-gap has opened, with the resistivity increasing close to exponentially until starting to flatten out at ~ 2 K. The magnetoresistance goes as H^2 and at low temperatures we observe Shubnikov-de Haas oscillations.

Search for Metamagnetic Transitions in the Cuprate Magnetic Cluster Compounds $\text{RbNa}_5\text{Cu}_4\text{As}_4\text{O}_{16}\text{C}_{12}$ and NaCuAsO_4

Clayhold, J.A., Clemson Univ., Physics and Astronomy

Hwu, S.-J., Clemson Univ., Chemistry

Zhou, W., Clemson Univ., Materials Science

The two cuprate cluster systems we have studied, $\text{RbNa}_5\text{Cu}_4\text{As}_4\text{O}_{16}\text{C}_{12}$ and NaCuAsO_4 , are essentially quasi-zero dimensional analogs of the well-known high- T_c cuprates. $\text{RbNa}_5\text{Cu}_4\text{As}_4\text{O}_{16}\text{C}_{12}$ is a two-dimensional, layered compound with a square-planar arrangement of covalently bonded copper and oxygen ions. The 2D planes are composed of square units (tetramers) of Cu_4O_4 which form a cluster

of 4 spins. The copper valence state is $2+$, so the Cu ions are magnetic with spin $1/2$. What distinguishes $\text{RbNa}_5\text{Cu}_4\text{As}_4\text{O}_{16}\text{C}_{12}$ from the familiar cuprate superconductors is a novel in-plane magnetic frustration, which eliminates superexchange between neighboring tetramers. It is possible that this lattice structure might be unique in providing a 2D square planar lattice of frustrated superexchange pathways.

NaCuAsO_4 is a high temperature decomposition product of $\text{RbNa}_5\text{Cu}_4\text{As}_4\text{O}_{16}\text{C}_{12}$ in which the closed topology of tetramers is broken to form a non-collinear chain of four linked Cu ions. Our studies of the thermodynamics and magnetization of NaCuAsO_4 indicated the absence of long-range magnetic coupling, and that the magnetic response was dominated by the local magnetic levels of the cluster, with a spin-singlet state as the ground state.

Magnetization and specific heat studies of $\text{RbNa}_5\text{Cu}_4\text{As}_4\text{O}_{16}\text{C}_{12}$ had indicated that the material is highly frustrated, ordering via a weak oxygen-oxygen direct exchange process at $T=16$ K despite a high temperature Curie-Weiss parameter of -86 K.

At the NHMFL, we searched for high field metamagnetic transitions in fields up to 30 T at 1.6 K, using both AC susceptibility coils and cantilever susceptometry with negative results.

Colossal Magnetoresistant Materials: The Key Role of Phase Separation

Dagotto, E., NHMFL/FSU, Physics

Hotta, T., NHMFL

Moreo, A., NHMFL/FSU, Physics

The study of the manganese oxides, widely known as manganites, that exhibit the “Colossal” Magnetoresistance (CMR) effect is among the main areas of research within the area of Strongly Correlated Electrons. After considerable theoretical effort in recent years, mainly guided by computational and mean-field studies of realistic models, considerable progress has been achieved in understanding the curious properties of these compounds. These recent studies suggest that the ground states of manganite models tend to be

intrinsically inhomogeneous due to the presence of strong tendencies toward phase separation, typically involving ferromagnetic metallic and antiferromagnetic charge and orbital ordered insulating domains.

Calculations of the resistivity versus temperature using mixed states lead to a good agreement with experiments. The mixed-phase tendencies have two origins: (i) electronic phase separation between phases with different densities that lead to nanometer scale coexisting clusters, and (ii) disorder-induced phase separation with percolative characteristics between equal-density phases, driven by disorder near first-order metal-insulator transitions. The coexisting clusters in the latter can be as large as a micrometer in size. It is argued that a large variety of experiments reviewed in detail here contain results compatible with the theoretical predictions. The main phenomenology of mixed-phase states appears to be independent of the fine details of the model employed, since the microscopic origin of the competing phases does not influence the results at the phenomenological level. However, it is quite important to clarify the electronic properties of the various manganite phases based on microscopic Hamiltonians, including strong electron-phonon Jahn-Teller and/or Coulomb interactions.

Thus, several issues are discussed here from the microscopic viewpoint as well, including the phase diagrams of manganite models, the stabilization of the charge/orbital/spin ordered half-doped CE-states, the importance of the naively small Heisenberg coupling among localized spins, the setup of accurate mean-field approximations, the existence of a new temperature scale, T^* , where clusters start forming above the Curie temperature, the presence of stripes in the system, and many others. However, much work remains to be carried out, and a list of open questions is included here. It is also argued that the mixed-phase phenomenology of manganites may appear in a large variety of compounds as well, including ruthenates, diluted magnetic semiconductors, and others. It is concluded that manganites reveal such a wide variety of interesting physical phenomena that their detailed study is quite important for progress in the field of Correlated Electrons.

This research is expected to appear in *Physics Reports* in 2001.

High Field Magnetization and Magnetotransport Measurements in Perovskites Compounds

Gama, S., UNICAMP, Campinas, Brazil
Coelho, A.A., UNICAMP, Campinas, Brazil
Rivas-Padilla, E.P., UNICAMP, Campinas, Brazil

The materials of interest for these measurements were manganite ceramics of the perovskite structure presenting magnetoresistive effects. All samples were prepared by solid state reaction-sintering procedure.

Magnetization and resistivity measurements as a function of temperature down to 2.5 K and applied magnetic field up to 18 T were performed.

Three sets of samples have been measured. The first one comprises four samples with constant variance in the A site radii distribution at a value of 0.0015 \AA^2 , and average A radii varying from 1.2245 Å up to 1.2337 Å. The second set comprises four samples with constant variance of 0.0072 \AA^2 , with A radii varying from 1.2271 Å up to 1.2321 Å. Finally, the third set comprises six samples of base composition $\text{La}_{0.67}\text{Sr}_{0.33}\text{MnO}_3$ doped with the rare-earths Er and Gd.

For the first two sets of samples, the objective is to study the effect of size variation at the site A at constant variance on the transport and magnetic properties of these materials. For the third set of samples, the objective is to investigate the effect of rare earth doping in the transport and magnetic properties of the base material. The obtained results show a very consistent evolution of the magnetotransport properties with the A site size and with the rare-earth concentration.

Acknowledgements: The authors wish to acknowledge financial support from Conselho Nacional de Desenvolvimento Científico e Tecnológico – CNPq, through grant 910101/97-3.

Hall Effect and Specific Heat of the Rare Earth Diantimonides

Gamble, B.K., Clemson Univ., Physics
Tessema, G.X., Clemson Univ., Physics and
National Science Foundation
Kuo, Y.K., National Dong Hwa Univ., Taiwan
Canfield, P., Iowa State Univ., Ames National
Laboratory, Physics and Astronomy
Lacerda, A.H., NHMFL/LANL

We have measured the temperature dependence between 2.1 K and 150 K of the Hall coefficient (R_H) of the layered compound PrSb_2 . This measurement is a continuation of a systematic study that we are presently conducting on several compounds from the family of rare-earth diantimonides, namely: LaSb_2 , NdSb_2 , CeSb_2 , and SmSb_2 . AC and adiabatic heat capacity measurements have been completed on all of the compounds confirming the low temperature antiferromagnetic transitions in PrSb_2 , NdSb_2 , CeSb_2 , and SmSb_2 . A 0.3% change in heat capacity was also found in PrSb_2 at 100 K, consistent with the resistance anomaly reported previously by Bud'ko, *et al.*¹

Using the 20 T magnet at NHMFL/Los Alamos, we performed resistance, magnetoresistance, and Hall measurements on PrSb_2 . Fig. 1 shows the Hall voltage at 18 K for positive and negative field

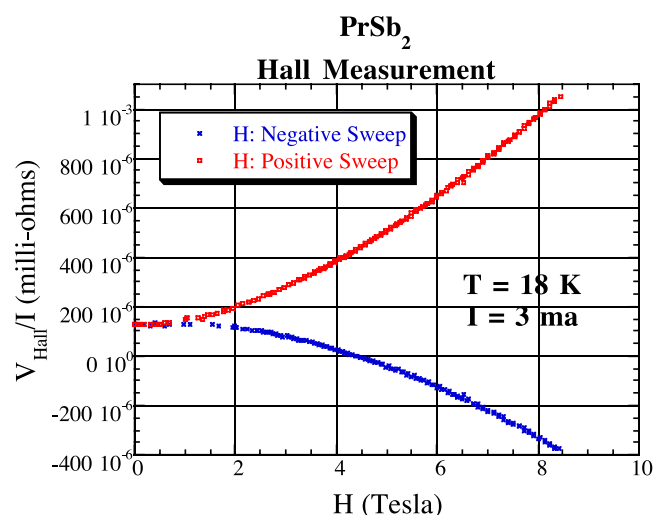


Figure 1. The Hall voltage of PrSb_2 for positive and negative field sweeps up to $H=10 \text{ T}$.

sweeps up to approximately $H=10 \text{ T}$. Analysis of the Hall coefficient throughout the temperature range previously mentioned confirms the results of earlier measurements which indicate up to 90% carrier condensation at $T = 5 \text{ K}$.

Acknowledgements: Work completed at the NHMFL was performed under the auspices of NSF, the State of Florida, and the U.S. Department of Energy.

¹ Bud'ko, S.L., *et al.*, Phys. Rev. B, **57**, 13624-12638 (1998).

Search for Field Induced Magnetic Transitions in R_2RuO_5 ($\text{R}=\text{Gd}$ and Tb)

■ IHRP ▲

Guertin, R.P., Tufts Univ., Physics and Astronomy
Cao, G., NHMFL
Crow, J.E., NHMFL
Mielke, C.H., NHMFL/LANL

The new ternary oxide system, R_2RuO_5 , contains two types of quite dissimilar magnetic constituents, rare earths and the 4d transition metal, Ru. Both Gd_2RuO_5 and Tb_2RuO_5 undergo magnetic ordering, at $T_M=8 \text{ K}$ and 18 K , respectively, and despite being semiconductors with large electrical resistivities at low temperature, they both show a very large linear term in the heat capacity. Isothermal magnetization measurements to 12 T for $T \ll T_M$ show several weak field induced magnetic transitions on the approach to magnetic saturation. The magnetic saturation for Tb_2RuO_5 falls short of the free ion value due to crystal field splitting of the R ion ground state.

The aim of the very high, pulsed field measurements was to try to observe even higher field-induced transitions as a way to more fully understand and quantify the crystal field interaction strength. Pulsed field magnetization measurements were carried in fields to 60 T using the short pulse magnets at FBNML/LANL. A magnetometer featuring lithographically etched pickup coils, designed originally by the R. Clark group from Australia, was used for all measurements.

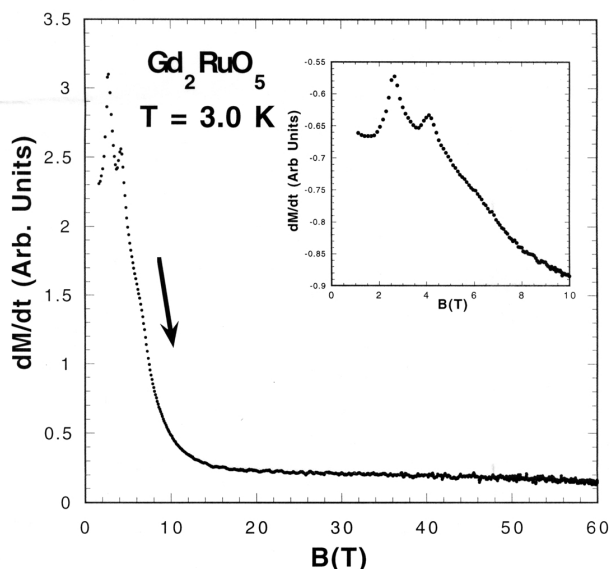


Figure 1. Pulsed field magnetization data to 60 T for Gd_2RuO_5 at 3 K. Inset shows detail of low field transitions in a 10 T pulse.

The data (see figure) clearly indicated a sequence of low (<7 T) field induced transitions, but no higher field transitions, thus setting a lower limit (≈ 100 K) on the crystal field interaction strength for the lowest lying R levels. The temperature dependence of the transitions was measured up to about 20 K, thereby testing the temperature stability of the magnetometer. The results have been submitted for publication as part of a comprehensive study of the magnetic, transport, and thermal properties of R_2RuO_5 .

Acknowledgements: This work was supported by NSF, cooperative agreement No. DMR95-27035, and the State of Florida. RPG was supported in part by the Research Corporation.

Low Energy Excitations in Impurity Substituted CuGeO_3

Jones, B.R., State Univ. of New York at Binghamton, Chemistry

Sushkov, A.B., SUNY-Binghamton, Chemistry

Musfeldt, J.L., SUNY-Binghamton, Chemistry

Wang, Y.J., NHMFL

Dhalenne, G., Universite de Paris-Sud, Laboratoire de Chimie des Solides

Revscolevschi, A., Universite de Paris-Sud, Laboratoire de Chimie des Solides

We report far-infrared reflectance measurements of Zn and Si doped CuGeO_3 single crystals as a function of applied magnetic field at low temperature. Overall, the low-energy far-infrared spectra are extraordinarily sensitive to the various phase boundaries in the H-T diagram with the features being especially rich in the low-temperature dimerized state. Zn doped reflectance ratio data is shown below. Zn impurity substitution rapidly collapses the 44 cm^{-1} spin gap, although broadened magnetic excitations are observed at the lightest doping level (0.2%) and a remnant is still observable at 0.7% substitution. In a similar (0.7%) Si doped sample, there is no evidence of the spin gap. Impurity substitution effects on the intensity of the 98 cm^{-1} zone-folding mode are striking as well. The lightly doped Zn crystals display an enhanced response and even at intermediate doping levels, the mode intensity is larger than that in the pristine material. The Si doped sample also displays an increased intensity of the 98 cm^{-1} mode in the spin Peierls phase relative to the pure material. The observed trends are understood in terms of the effect of disorder on the spin gap and 98 cm^{-1} mode.

Acknowledgements: We are grateful for financial support from the Materials Science Division at the U.S. Department of Energy (DE-FG02-99ER45741) and the Division of Materials Science at the National Science Foundation (DMR-9623221).

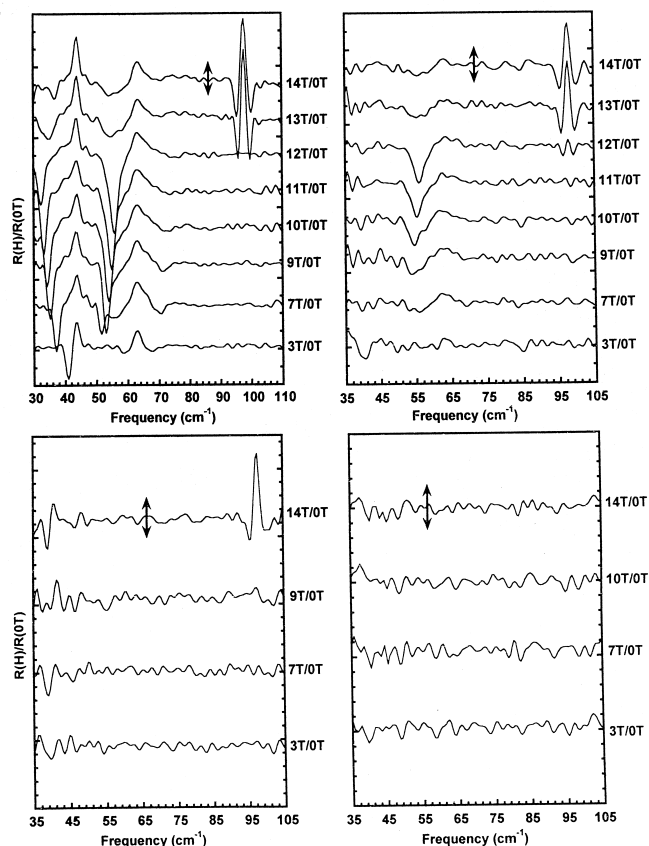


Figure 1. Reflectance ratio spectra of CuGeO_3 as a function of applied field at several different levels of Zn doping: 0.2%, 0.7%, 1.5%, and 4%.

Magnetic Field Dependent Optical Studies of a Layered Antiferromagnet $\text{Pr}_{1/2}\text{Sr}_{1/2}\text{MnO}_3$

Jung, J.H., Seoul National Univ. (SNU)-Korea,
Center for Strongly Correlated Material Research
Lee, H.J., SNU-Korea, Physics
Noh, T.W., SNU-Korea, Physics
Moritomo, Y., Nagoya Univ.-Japan, Applied Physics
Wang, Y.J., NHMFL
Wei, X., NHMFL

Doped manganites with chemical formula $\text{R}_{1-x}\text{A}_x\text{MnO}_3$ ($\text{R}=\text{La}, \text{Pr}, \text{Nd}$ and $\text{A}=\text{Ca}, \text{Sr}, \text{Ba}$) have attracted much attention due to their exotic electrical and magnetic properties. Among them, physical properties of $\text{Pr}_{1/2}\text{Sr}_{1/2}\text{MnO}_3$ seem to be quite interesting, since it is known as the “A-type” antiferromagnet. In this spin configuration, spins in the layer will be ferromagnetically ordered but spins between the layers are antiferromagnetically

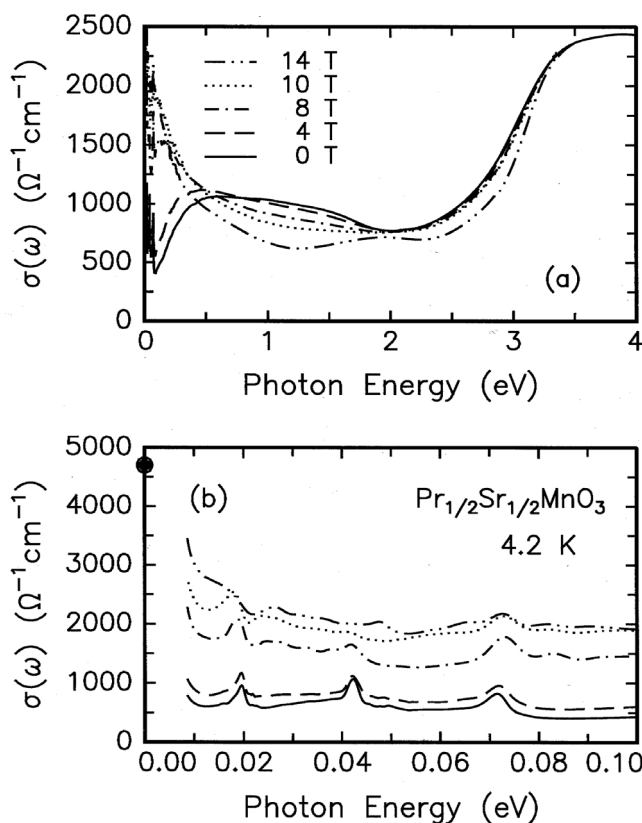


Figure 1. H-dependent $\sigma(\omega)$ of $\text{Pr}_{1/2}\text{Sr}_{1/2}\text{MnO}_3$ below (a) 4.0 eV and (b) 0.1 eV during the H-increasing run. In (b), the solid circle represents the DC conductivity value at 14.0 T.

ordered.¹ Then, it will have a metallic conduction in the layer, so its transport should have a 2-dimensional (2D) nature. Under a high magnetic field (H), the long range spin ordering will be disturbed and 3D metallic conduction will become possible. In spite of this fascinating dimensional crossover from 2D to 3D, optical investigations on the layered antiferromagnetic materials have been rare.

Using Bruker and McPherson spectrometers in the NHMFL, we measured reflectivity spectra of $\text{Pr}_{1/2}\text{Sr}_{1/2}\text{MnO}_3$ under various magnetic fields ($H=0\sim 14$ T). Using the Kramers-Kronig analysis, the optical conductivity spectra $\sigma(\omega)$, shown in Fig. 1, were obtained. At 0.0 T, there are broad peaks around 1.0 and 4.0 eV. As H increases, the spectral weights near 1.0 and 3.0 eV are transferred to a lower energy region. The low frequency details of transferred spectral weights below 0.1 eV can be seen in Fig. 1 (b). At 0.0 T, there are sharp peaks due to the optical phonon modes and a hint of a small rise in $\sigma(\omega)$ in the low frequency limit, suggesting the

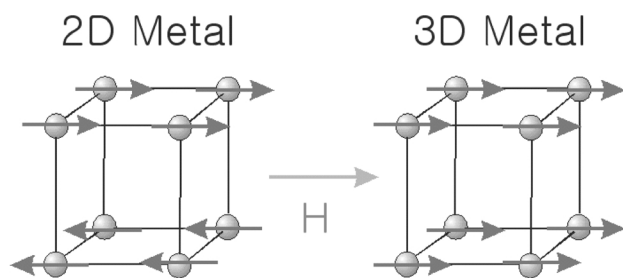


Figure 2. A schematic diagram of the dimensional crossover from 2D to 3D by the application of external magnetic field (H).

existence of a small Drude-like peak. As H increases, the Drude-like peak becomes more clear below 0.04 eV. The solid circle represents the DC conductivity value at 14.0 T. Therefore, $\sigma(\omega)$ below 0.1 eV at high H should be viewed as two parts, i.e., the Drude and the large incoherent absorption peaks. A similar mid-infrared incoherent absorption peak has been observed in many manganites and attributed to incoherent polaron or orbital fluctuation. However, from the temperature dependent $\sigma(\omega)$ of this compound, we were able to show that the mid-infrared peak originated from the polaron absorption.²

Increases of the Drude weights and the incoherent polaron absorption with H can be explained by the dimensional crossover from 2D to 3D, as shown in Fig. 2. In $H=0.0$ T, the carriers will move within the ferromagnetic layer and the carrier motion along the layers will be prohibited. Then, carrier motion in 2D will give rise to a small Drude weight and polaron absorption. However, at high H , spins are ferromagnetically aligned for all directions. Then carrier motion in 3D will give rise to a large Drude weight and polaron. When we calculated the sum of the coherent and incoherent polaron absorption, we found that the sum of polaron absorptions at high H was increased by the amount of 3/2 as compared with that at 0.0 T.³ These results suggested the occurrence of the dimensional crossover from 2D to 3D metal by the strong magnetic field in the layered antiferromagnet $\text{Pr}_{1/2}\text{Sr}_{1/2}\text{MnO}_3$.

¹ Kawano, H., *et al.*, Phys. Rev. Lett. **78**, 4253 (1997).

² Jung, J.H., *et al.*, Phys. Rev. B. **61**, 14 656 (2000).

³ Jung, J.H., *et al.*, Phys. Rev. B. **62**, 8634 (2000).

Magnetization Step in the Molecule-Based Magnet $\text{Fe}[\text{N}(\text{CN})_2]_2$

Kmety, C.R., Ohio State Univ., Physics¹

Epstein, A.J., Ohio State Univ., Physics and Chemistry

This work is the continuation of our study² of field-induced magnetic properties in $\text{Fe}[\text{N}(\text{CN})_2]_2$ by DC magnetization, using the NHMFL cantilever beam magnetometer ($T=25$ mK, $0 \leq H \leq 17.5$ T), and vibrating sample magnetometer ($2 \leq T \leq 4.2$ K, $0 \leq H \leq 30$ T). Based on earlier studies, the isothermal (5 K) magnetization $M(H)$ reached only a value of about $M(5.5 \text{ T}) \approx 1 \mu_B$,³ which is much lower than $4 \mu_B$, corresponding to a $J=2$ with $g_J=2$. As the applied magnetic field was increased above 5.5 T, the isothermal (45 mK) AC susceptibility, $\chi'(H)$, revealed a peak at the critical field $H_{cr} \approx 8.7$ T.² The low value of $M(H)$ at 5.5 T and the peak in $\chi'(H)$ at 8.7 T motivated us to search for a step in the DC magnetization.

The vibrating sample magnetometer results uncovered a step in the DC magnetization ($M(H)$) at the critical field $H_{cr} \approx 8.7$ T (see Fig. 1), which appeared to be independent of temperature and sweep rate. The cantilever beam magnetometer confirmed a change in the magnetization at about 8.7 T. The magnetization

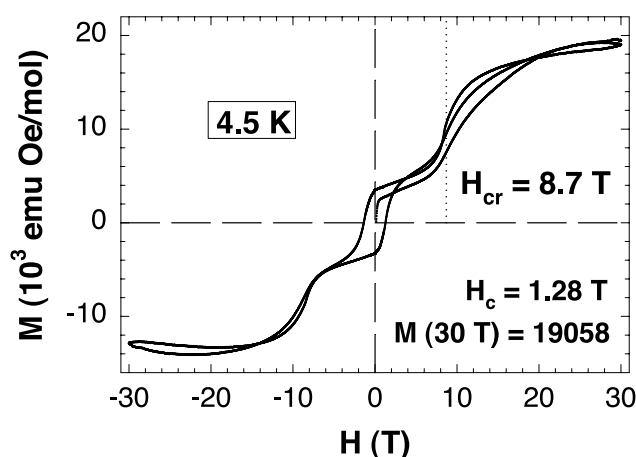


Figure 1. Isothermal magnetization as a function of applied magnetic field measured with the vibrating sample magnetometer for $\text{Fe}[\text{N}(\text{CN})_2]_2$. The plot summarizes the critical field (H_{cr}), the coercive field (H_c), and the magnetization at 30 T ($M(30 \text{ T})$).

step in the antiferromagnetically ordered $\text{Fe}[\text{N}(\text{CN})_2]_2$ can be explained by a field-induced crossing of the energy levels of the Fe^{2+} ions, which is similar to the crossing of the energy levels in high-spin clusters such as Mn_{12} and Fe_8 . The value of the critical field allows the estimation of the magnitude of the axial zero-field splitting parameter D , which gives insight into the strength of the magnetic anisotropy in the system.

Acknowledgements: This work was supported by the DOE (Grant No. DE-FG02-86ER45271).

¹ Present address: Materials Science Division, Argonne National Laboratory.

² Kmety, C.R., *et al.*, 1999 NHMFL Annual Research Review.

³ Kmety, C.R., Ph.D. Thesis, Ohio State University, 2000.

Magnetization of Low Dimensional Quantum Heisenberg Antiferromagnets

Landee, C.P., Clark Univ., Physics
Jensen, W.E., Clark Univ., Physics
Woodward, F.M., Clark Univ., Physics
Turnbull, M.M., Clark Univ., Chemistry

We have been exploring a class of one dimensional $S = 1/2$ quantum Heisenberg antiferromagnets (QHAF) by examining a parent compound $\text{Cu}(\text{pz})(\text{NO}_3)_2$ and its variants. The copper pyrazine family of magnets has been extended by attaching one or two methyl groups to the pyrazine molecule, which substantially alters the magnetic interaction strength ($|J| \approx 10$ K) while retaining the one-dimensional character. Fig. 1 shows five sets of data collected at the NHMFL over a period of several years. The most recent data were collected this year on a 30 T Bitter magnet using a vibrating sample magnetometer (VSM). These data represent the completion of all unique methyl and dimethyl substituted copper pyrazine magnets. The upward curvature in the magnetization data before saturation is the hallmark¹ of a 1D QHAF. The saturation fields are 18 T and 19 T for the 2,5- and 2,6-dimethylpyrazine compounds, respectively, which is direct proof of the variation of magnetic exchange among these compounds.

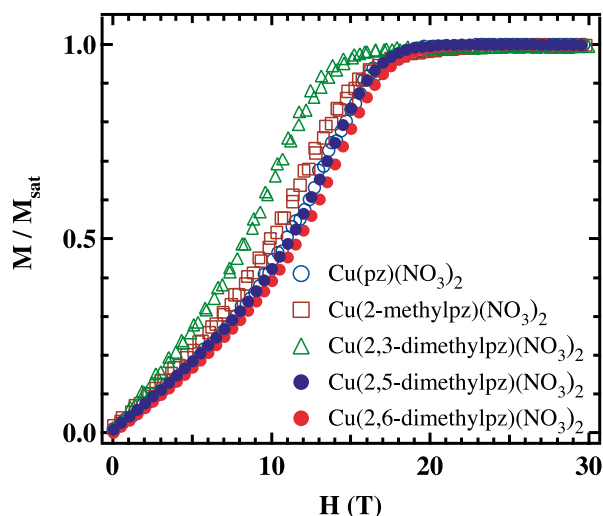


Figure 1. 1D QHAF at $T = 2.0$ K.

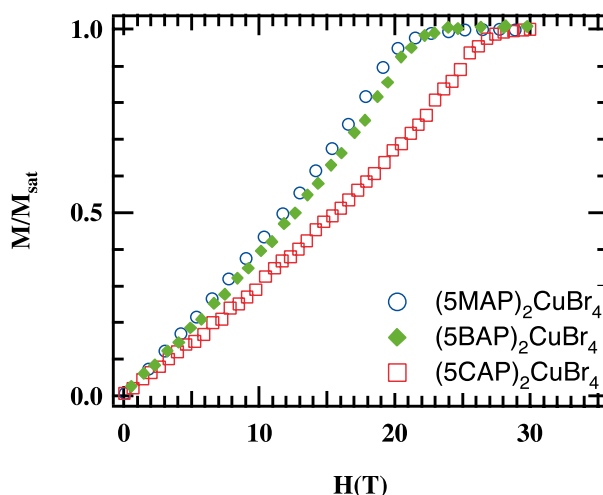


Figure 2. 2D QHAF at $T = 2.0$ K.

We have also expanded the catalog of 2D $S = 1/2$ QHAF, based upon the structural motif $(5\text{SAP})_2\text{CuBr}_4$, where 5SAP represents 2-amino-5S-pyridinium. The 5S substituent can be chlorine, methyl, or now, bromine. The magnetization data collected on the NHMFL VSM this year completes the family of 2D copper tetrabromides with a saturation field of 18 T for the newly synthesized $(5\text{BAP})_2\text{CuBr}_4$ compound. These data represent the first saturation magnetization curves of a 2D QHAF system and show the distinct curvature predicted for the 2D QHAF magnetization curve.²

¹ Bonner, J.C., *et al.*, Phys. Rev., **135**, A640, (1964).

² Zhitomirsky, M.E., *et al.*, Phys. Rev. B, **57**, 5013 (1998).

Magnetization Measurements of New $S=1/2$ Antiferromagnetic Spin-Ladder Compounds

Landee, C.P., Clark Univ., Physics
Turnbull, M.M., Clark Univ., Chemistry
Galeriu, C., Clark Univ., Physics
Giantsidis, J., Clark Univ., Chemistry
Woodward, F.M., Clark Univ., Physics

We are investigating the properties of some new $S=1/2$ Heisenberg antiferromagnetic low dimensional compounds, with the goal of understanding the influence of quantum effects on the magnetic behavior. It is essential, for these effects to be observed, to make measurements at low temperatures and high magnetic fields.

More experimental systems are needed in order to test and improve the theoretical predictions for systems with interacting fermions. We have synthesized and studied two new spin-ladder compounds: $(5\text{IAP})_2\text{CuBr}_4 \cdot 2\text{H}_2\text{O}$ and $(5\text{NAP})_2\text{CuBr}_4 \cdot \text{H}_2\text{O}$ ($5\text{IAP} = 5\text{-iodo, 2-aminopyridinium}$ and $5\text{NAP} = 5\text{-nitro, 2-aminopyridinium}$). These compounds¹ consist of CuBr_4 tetrahedra, packed into ladders, and isolated by the organic groups. The exchange interactions

occur through Br-Br direct contacts, and are low enough ($J_{\text{rung}} \sim 13$ K, $J_{\text{rail}} \sim 1$ K for the iodo compound; $J_{\text{rung}} \sim 25$ K, $J_{\text{rail}} \sim 13$ K for the nitro compound) to allow us to fully saturate the magnetization. This way we are able to reach and investigate a very interesting quantum critical point,² where the ground state changes at the critical field. The critical field for the nitro compound exceeds 30 T, and is being studied in pulsed fields at LANL.

¹ Landee, C.P., *et al.*, preprint, cond-mat/0011016.

² Sachdev, S., *Quantum Phase Transitions*, Cambridge University Press, Cambridge, MA, (2000).

Resistivity of Mixed-Phase Manganites

■ IHRP ■

Mayr, M., NHMFL
Moreo, A., NHMFL/FSU
Verges, J., Instituto de Ciencias de Materiales de Madrid, Spain
Arispe, J., NHMFL
Feiguin, A., NHMFL
Dagotto, E., NHMFL/FSU

The resistivity of manganites is studied using a random-resistor network, based on phase separation between metallic and insulating domains. When percolation occurs, both as chemical composition or temperature vary, results in good agreement with experiments are obtained. Similar conclusions are reached using quantum calculations and microscopic considerations. Above the Curie temperature, it is argued that ferromagnetic clusters should exist in Mn oxides. Small magnetic fields induce large resistivity changes and a bad-metal state with (disconnected) insulating domains.

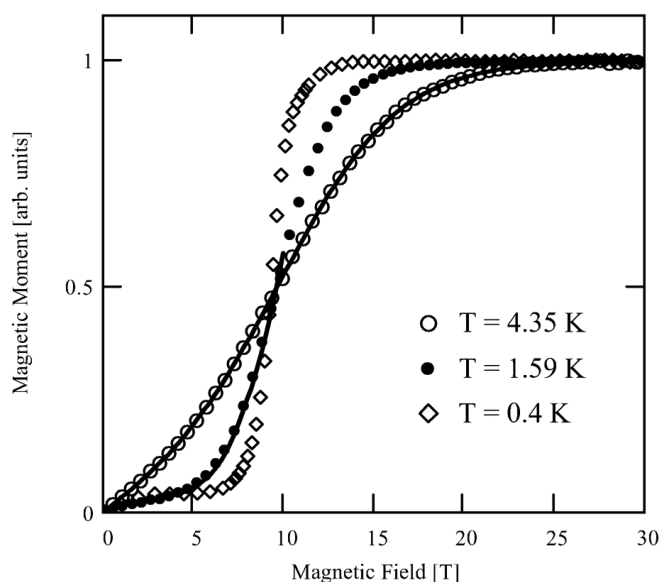


Figure 1. High field magnetization curve for different temperatures for $(5\text{IAP})_2\text{CuBr}_4 \cdot 2\text{H}_2\text{O}$. Data taken at NHMFL. Only representative points have been plotted.

Unusual Thermodynamic Properties of Lanthanide Ruthenates

McCall, S., NHMFL

Zhou, Z.X., NHMFL

Alexander, C.S., NHMFL

Cao, G., NHMFL

Crow, J.E., NHMFL

Guertin, R.P., Tufts Univ., Physics and Astronomy

Mielke, C.H., NHMFL/LANL

There has been an increasingly intensive research effort in recent years toward understanding the physical properties of layered 4d- and 5d-transition metal oxides, which show a large variety of unexpected physical phenomena.¹ There appear to be relatively few examples in the literature, however, of oxides with both 4d or 5d transition metals, and rare earth constituents, which are believed to be rich in physics. As an effort to fill this void, we have recently broadened our research scope to include studies of materials containing 4d- and 4f-electrons with non-perovskite structures. Polycrystalline and single crystal samples of the lanthanide ruthenate series Ln_2RuO_5 ($\text{Ln}=\text{Pr}$, Nd , Sm , Gd and Tb)² and Ln_3RuO_7 (Pr , Nd , Sm , Gd and Tb) have systematically been investigated. All results indicate a critical role played by 4d-electrons that chiefly govern physical properties.

Ln_2RuO_5 . Ln_2RuO_5 has a complex orthorhombic structure (space group Pnma) possessing chains of

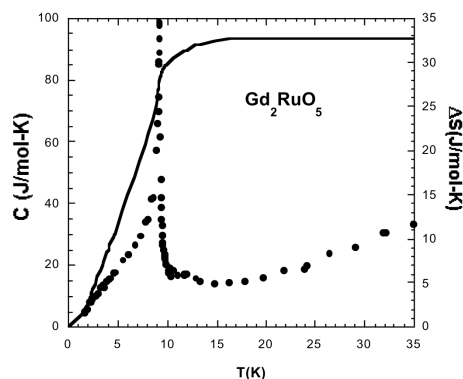


Figure 1. The heat capacity of Gd_2RuO_5 (left axis) shows the ordering of the Gd ions just below 10 K. The line shows the ΔS removed (right axis) by this ordering after subtracting the high temperature fit to this data ($C=\gamma T+\beta T^3$). The entropy removed under the peak corresponds to 96% of the expected spin entropy for the Gd.

RuO_5 pyramids that are corner-sharing and two inequivalent seven coordinated Ln sites that are edge-sharing. These materials magnetically order in the range $8 < T < 24$ K with the ordering involving both the Ln and Ru cations. At T_M , a weak ferromagnetic moment emerges upon cooling, most likely due to a canted antiferromagnetic spin configuration. The striking feature of these systems is characterized by the low temperature linear specific heat coefficient, γ , that is anomalously large, ranging from $\gamma=229$ to 774 mJ/mole-K^2 , for $\text{Ln}=\text{Nd}$ and $\text{Ln}=\text{Gd}$, respectively (see Fig.1). These values are comparable to those for heavy fermion systems, yet all five members of the Ln_2RuO_5 series exhibit semiconducting to insulating behavior. Isomorphic Gd_2TiO_5 , where Ti with no d-electrons ($4d^0$ configuration) replaces Ru ($4d^4$ configuration), has a vanishingly small γ , indicating that the thermodynamic properties of Ln_2RuO_5 are dominated by 4d electrons. The 4d electrons significantly enhance the Ln-Ln interaction, as demonstrated by the dramatic increase in ordering temperature for Gd_2RuO_5 ($T_M=9$ K), compared to Gd_2TiO_5 which does not appear to order magnetically at least above 1.5 K.

Ln_3RuO_7 . Ln_3RuO_7 features chains of corner-shared octahedra of RuO_6 along the c-axis. These chains facilitate a strong exchange interaction between Ru ions. Unlike in Ln_2RuO_5 , where the valence state of the Ru ion is $4+$, the oxidation state in La_3RuO_7 is $5+$, thus $S=3/2$. These materials are magnetic insulators characterized by two magnetic ordering temperatures with one being closely associated with d-electrons and the other with f-d electron coupling. Pr_3RuO_7 shown in Fig.2, for example, antiferromagnetically orders at $T_{N1}=55$ K and $T_{N2}=36$ K. Substituting Nb^{5+} ($4d^0$) for Ru^{5+} rapidly suppresses T_{N1} and T_{N2} .

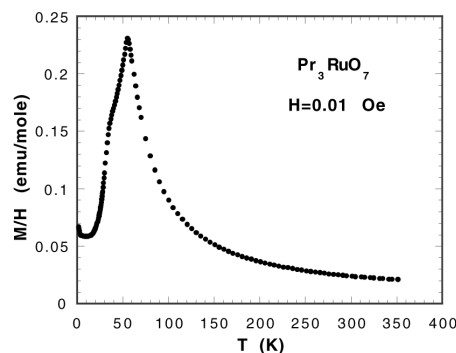


Figure 2. Magnetic susceptibility of Pr_3RuO_7 showing a peak at $T_{N1}=55$ K and a change in slope representing $T_{N2}=36$ K.

whereas, La doping for Pr only results in a drop in T_{N2} with T_{N1} remaining essentially unchanged. Similar to what has been observed in Ln_2RuO_5 , the Ru ions precipitate and promote ordering among rare earth ions, clearly enhancing their exchange interaction. This point is further supported by paramagnetic behavior seen in Pr_3NbO_7 where Nb^{5+} has no d-electrons. Remarkably, Ln_3RuO_7 shows no large linear coefficient of the heat capacity comparable to that observed in Ln_2RuO_5 . This sharp difference highlights the uniqueness of the anomalously large γ observed in Ln_2RuO_5 . The lanthanide ruthenates, which are a significant addition to the family of magnetic oxides, once again reveal a glimpse of the rich and yet complex 4d-electron oxides.

¹ Cao, G., *et al.*, Phys. Rev. Lett., **78**, 1751 (1997); Cao, G., *et al.*, Phys. Rev. B, **56**, 321 (1997); Guertin, R.P., *et al.*, "Proc. Physical Phenomena at High Magnetic Fields III", ed. by Z.Fisk, *et al.*, World Scientific, 1999; Cao, G., *et al.*, Material Science and Engineering B., **36**, 76 (1999); Cao, G., *et al.*, Phys. Rev. B., **61**, R5053 (2000).

² Cao, G., *et al.*, Phys. Rev. B., to be published, 2001.

High-Field Magnetization of the Magnetic Molecules $\{\text{Mo}_{72}\text{Fe}_{30}\}$ and $\{\text{Mo}_{12}\text{Ni}_4\}$

Modler, R., Ames Laboratory and Iowa State University, Physics and Astronomy

Luban, M., Ames Laboratory and Iowa State University, Physics and Astronomy

Kögerler, P., Ames Laboratory and Iowa State University, Physics and Astronomy

Canfield, P., Ames Laboratory and Iowa State University, Physics and Astronomy

Bud'ko, S., Ames Laboratory and Iowa State University, Physics and Astronomy

Harrison, N., NHMFL/LANL

Lacerda, A., NHMFL/LANL

Due to the recent successes in polyoxomolybdate chemistry, complex magnetic molecules are available in high-quality single-crystal form and macroscopic quantities. In these materials, high magnetic fields at low temperatures provide an ideal tool for determining the properties of the low-lying states and additionally enable the experimental determination of field induced energy-level crossings. We performed

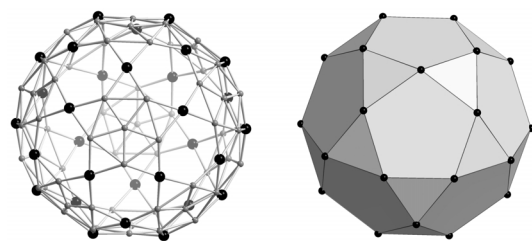


Figure 1. Representation of the metal skeleton in $\{\text{Mo}_{72}\text{Fe}_{30}\}$ (left) and the icosidodecahedron formed by the 30 Fe positions (right).

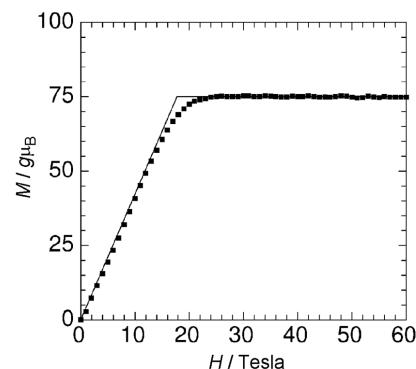


Figure 2. Magnetization vs. B for $\{\text{Mo}_{72}\text{Fe}_{30}\}$ at 0.46 K (expt. values: black squares, theoretical curve: solid line).

measurements on two different magnetic molecules, $\{\text{Mo}_{72}\text{Fe}_{30}\}$ ¹ and $\{\text{Mo}_{12}\text{Ni}_4\}$.²

The magnetic molecule $\{\text{Mo}_{72}\text{Fe}_{30}\}$ contains 30 Fe^{3+} ions ($s=5/2$) located on the vertices of an Archimedean polytope, the icosidodecahedron (Fig. 1). Antiferromagnetic exchange between Fe ions gives rise to symmetric frustrated magnetic spin arrangement at low temperatures, as predicted by our classical and quantum Heisenberg model calculations. Utilizing a 60 T pulsed magnet at Los Alamos, we were able to confirm the low-temperature predictions for the magnetization as a function of magnetic field. We observed a linear rise of the magnetization ($T=0.46$ K) up to a field of about 18 T above which the magnetization saturates at the expected value of 75 $g\mu_B$ per molecule (Fig. 2).

The tetrahedral array of four Ni^{2+} ($s=1$) ions in $\{\text{Mo}_{12}\text{Ni}_4\}$ interact via isotropic antiferromagnetic exchange. Our theoretical studies, based on the Heisenberg model, predict the occurrence of level crossings associated with steps in the magnetization at certain discrete values of B. First measurements

have been performed at 0.44 K and these confirm the predicted level crossings.

¹ $\{\text{Mo}_{72}\text{Fe}_{30}\} = [\text{Mo}_{72}\text{Fe}_{30}\text{O}_{252}(\text{CH}_3\text{COO})_{12}(\text{Mo}_2\text{O}_7(\text{H}_2\text{O}))_2(\text{H}_2\text{Mo}_8\text{O}_9(\text{H}_2\text{O}))(\text{H}_2\text{O})_{91}]$; Müller, A., *et al.*, *Angewandte Chemie, International Edition*, **38**, 3238-3241 (1999).

² $\{\text{Mo}_{12}\text{Ni}_4\} = [\text{H}_2\text{Mo}_{12}\text{Ni}_4\text{O}_{30}(\text{OH})_{10}(\text{H}_2\text{O})_{12}]$; Müller, A., *et al.*, *Inorganic Chemistry*, **39**, 5176-5177 (2000).

Fermi Surface and Spectral Functions of a Hole Doped Spin-Fermion Model for Cuprates

Moraghebi, M., NHMFL

Buhler, C., NHMFL

Yunoki, S., Univ. of Groningen, The Netherlands, Physics

Moreo, A., NHMFL

Using numerical techniques, we study the spectral function $A(\mathbf{k}, \omega)$ of a spin-fermion model for cuprates in the regime where magnetic and charge domains (stripes) are developed upon hole-doping. From $A(\mathbf{k}, \omega)$ we study the electronic dynamics and determine the fermi surface (FS), which is compared with angular resolved photoemission results for $\text{La}_{1-x}\text{Sr}_x\text{CuO}_2$. A pseudogap is observed in the density of states at the chemical potential for all finite dopings. The striped ground state appears to be metallic in this model since there is finite spectral weight at the chemical potential, but the electronic hopping seems to be stronger perpendicular to the stripes rather than along them.

The band structure is not rigid, contrary to the behavior found in mean-field studies, and changes with doping. Both mid-gap (stripe induced) and valence band states determine the FS. For vertical (horizontal) stripes, a clear FS appears close to $(\pi, 0)$ ($(0, \pi)$), while no FS is observed close to $(0, \pi)$ ($(\pi, 0)$). Along the diagonal direction the spectral function shows a clear quasi-particle peak close to $(0, 0)$, but its weight is reduced as the chemical potential is approached. A weak FS develops along this direction as the system is doped.

Magnetization Measurements on the III-VI Diluted Magnetic Semiconductor $\text{Ga}_{1-x}\text{Mn}_x\text{S}$ at High Fields

Pekarek, T.M., Univ. of North Florida, Natural Sciences

Maymi, C., Univ. of North Florida, Natural Sciences

Scott, T., Univ. of North Florida, Natural Sciences

Elerbee, J., Univ. of North Florida, Natural Sciences

Crooker, B.C., Fordham Univ., Physics

Miotkowski, I., Purdue Univ., Physics

Ramdas, A.K., Purdue Univ., Physics

The new class of layered III-VI Diluted Magnetic Semiconductors (DMS) have a two-dimensional structure (similar to mica) and complement the enormous progress in the II-VI DMS and the more recent efforts in the Mn doped III-V DMS systems. The III-VI semiconductors GaSe, InSe, and GaTe have received considerable interest in the last few years because they have remarkable nonlinear optical properties and are promising materials for photoelectronic applications. GaS is comparatively uninvestigated and, to our knowledge, no work has been reported on Mn in GaS.

Little is known about the magnetic properties of this new class of layered III-VI DMS except for a pair of publications^{1,2} that presents magnetization data in fields below 6 T on $\text{Ga}_{1-x}\text{Mn}_x\text{Se}$ and $\text{Ga}_{1-x}\text{Mn}_x\text{S}$, respectively. The prominent broad peak from 119 to 195 K in $\text{Ga}_{1-x}\text{Mn}_x\text{Se}$, ascribed to direct Mn-Mn pairs, is absent in $\text{Ga}_{1-x}\text{Mn}_x\text{S}$. In this temperature range, $\text{Ga}_{1-x}\text{Mn}_x\text{S}$ is Curie-Weiss, like with $J_{\text{eff}}/k_B = -50$ K. $\text{Ga}_{1-x}\text{Mn}_x\text{S}$ shows a cusp at 10.9 K for an $x=0.066$ sample similar to the spin-glass transition observed in the II-VI DMS.

Magnetization measurements on a nominal $x=0.05$ $\text{Ga}_{1-x}\text{Mn}_x\text{S}$ crystal ($m=0.0023$ g) were made at the NHMFL in fields up to 25 T using the cantilever method and are shown in Fig. 1. The set temperatures are from 20 to 70 K and are above the spin-glass like cusp previously reported near 10 K. These measurements were calibrated by regulating a current through a wire loop attached to the cantilever. An instrumental artifact due to a mechanical bi-stability

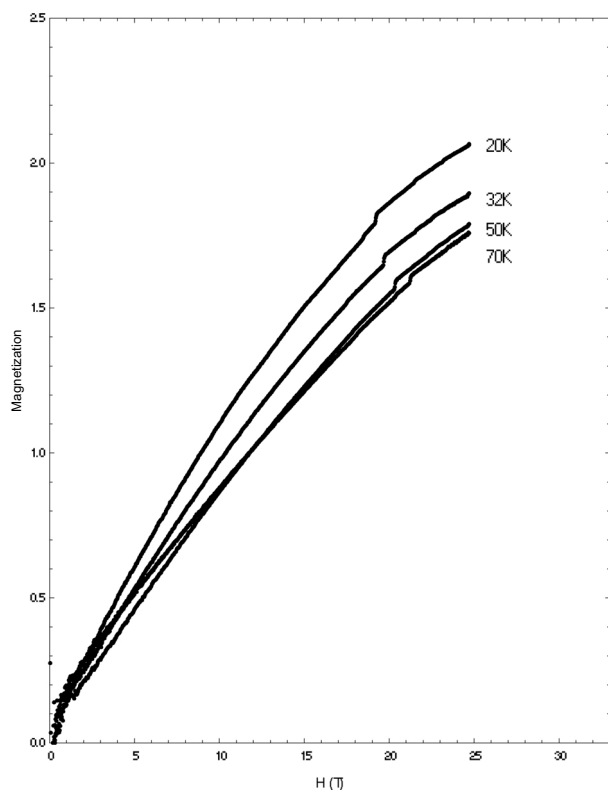


Figure 1. Magnetization versus field data for a 0.0023 g $\text{Ga}_{1-x}\text{Mn}_x\text{S}$ crystal at 20, 32, 50, and 70 K in fields up to 25 T.

in the cantilever was identified, characterized, and subtracted from the data. These measurements show the magnetization saturates significantly slower than a standard paramagnetic and suggests that the ground multiplet for the singlet Mn ions has an energy/ k_B gap around 20 K between a non-magnetic ground state and magnetic excited states. Theoretical work is underway to investigate the underlying energy levels that give rise to the observed magnetic behavior in this new layered III-VI DMS system.

Acknowledgements: This research was supported by Cottrell College Science Awards CC4719, CC4845, and CC4668 from Research Corporation, by the Florida Space Grant Consortium, and by NSF Grants No. DMR-92-21390, DMR-94-00415, DMR-99-72196, and DMR-99-75887.

¹ Pekarek, T.M., *et al.*, J. Appl. Phys., **83**, 7243 (1998).

² Pekarek, T.M., *et al.*, J. Appl. Phys., **87**, 6448 (2000).

Magnetoresistance of $\text{ErNi}_2\text{B}_2\text{C}$

Schmiedeshoff, G.M., Occidental College, Physics
 Beyermann, W.P., Univ. of California, Physics
 Lacerda, A.H., NHMFL/LANL
 Canfield, P.C., Iowa State Univ., Ames National
 Laboratory, Physics and Astronomy

We have measured the transverse magnetoresistance of a single crystal of $\text{ErNi}_2\text{B}_2\text{C}$, a compound that becomes a superconductor near 11 K, enters an antiferromagnetic state near 6 K, and a ferromagnetic state near 2.5 K.¹ Our results complement and extend lower field results in the literature.²

The magnetoresistance is anisotropic as one would expect for a magnetic, tetragonal compound. Above T_c the magnetoresistance is positive and quadratic with the field aligned along the [001] axis. With fields along the [100] axis, however, the magnetoresistance is negative and exhibits a broad minimum near 10 T. This behavior suggests that the spin fluctuations responsible for the negative magnetoresistance are confined to the basal plane.

The transition to antiferromagnetism is clearly visible in our resistivity and magnetoresistance data. Earlier measurements have characterized the low-field dependence of T_N : saturating below about 2 T with fields along the [100] axis, but showing no significant field dependence with up to 2 T along the [001] axis [2]. We find that higher fields depress T_N quadratically with H along the latter axis. Extending the quadratic fit indicates that $T_N = 0$ at 17.1 T.

We saw no evidence of additional phase transitions (such as the ferromagnetic transition) in our data. A fuller description of our results will appear elsewhere.

¹ Schmiedeshoff, G.M., *et al.*, J. Superconductivity, **13**, 847 (2000).

² Cho, B.K., *et al.*, Phys. Rev. B, **52**, 3684 (1995); Bud'ko, S. *et al.*, Phys. Rev. B, **61**, 14932 (2000).

Automotive Paint Stabilization Study by EPR

Shatlock, M., PPG Industries
Maresch, G.G., NHMFL
Brunel, L.-C., NHMFL

The stabilization of polymers such as polyacrylics, polyurethanes and polyolefins involves the use of various types of additives. Automotive paints contain hindered-amin light stabilizers (HALS) as inhibitors of polymer photooxidation.¹ In the process of polymer exposure to light in the presence of oxygen, these lead to the formation of free nitroso radicals. These in turn react with radical sites on the polymers that form the backbone of the coating matrix. These polymer radicals are intermediates in the Dennisov cycle, a primary mechanism for degradation of the coating. The activated HALS in the nitroso form react with the polymer radical to form amino ethers, interrupting the Dennisov cycle. Subsequently, the amino ether degrades, leaving a nitroso radical and re-establishing the integrity of the polymer. Electron paramagnetic resonance (EPR) spectroscopy can provide quantitative analysis of nitroso radicals. It is of interest to measure the concentration of HALS as a function of weathering, either in a "weatherometer" or by exposure to the Florida sun, and also to measure this concentration versus depth from the surface of the coating in the clear film.

Clear coat thin microtomed slices have been studied by X-band EPR to determine the radical concentration as function of depth in the original paint layer. A reference sample of an indolinic nitroxide in polystyrene was used as a standard. Through the use of microtomy, slices of coating as small as five microns can be analyzed, providing a spacial location of HALS in a finished coating. The samples are swelled with methylene chloride prior to analysis in order to induce motional narrowing. Prior to oxidation the nitroso radical concentration in the clear coats are in the range of 500 μ molar. After oxidation treatment, the radical concentration increases strongly up to 40 fold or 20 mmolar dependent on sample depth.

The automotive paints age by loss of HALS content. The EPR results show that after six years of Florida sun exposure the clear coats can have a loss of nearly two orders of magnitude of the stabilizing additives. More experiments are in progress to examine the influence of which type of stabilizer is used and how the stabilizer loss varies with the specific conditions of weathering. When measured as a function of age, it has been suggested that this information is of value in predicting the overall durability of the coating to various weathering conditions.

Acknowledgements: This work was supported by NSF grant 5024-54522. The authors thank Prof. P. Fajer for access to his X-band spectrometer.

¹ Step, E.N., *et al.*, *Macromol.*, **27**, 2529 (1994).

HFEPR Spectroscopy of Metal Centers in Silicon Oxide Glasses

Shatlock, M., PPG Industries
Brunel, L.-C., NHMFL
Maresch, G.G., NHMFL

Selenium metal is added to silica glasses in the melt in certain formulas as a colorant. The material is added to counteract the gray color caused by the presence of Fe²⁺ ions that are added to absorb heat. Because of the volatility of Se the majority of it is lost on melting and retention of the metal in cooled glass is low. The situation is further complicated by the presence of sulfur since S and Se are both thought to interact with the iron. High-frequency electron paramagnetic resonance (HFEPR) spectroscopy is tested if it is able to obtain spectral differences from glass samples with different concentration of selenium. The question addressed is: can iron-selenium complexes be distinguished from iron-sulfur complexes exploiting the higher resolution as compared to conventional EPR.¹

EPR spectra acquired at conventional frequencies at X-band (10 GHz) and at high frequencies (220 GHz) show strong features from metal centers. At X-band

a very broad spectrum at $g_{\text{eff}} = 4.3$ is detected and originates from Fe^{3+} centers surrounded by oxygen in axially distorted octahedral and tetrahedral symmetry. A signal at $g_{\text{eff}} = 6.8$ which is known to relate to iron-sulfur complexes² has not been observed. Due to the dominant spin-orbit coupling which scales with the microwave frequency, the iron signals have not been detected at high frequencies. More interestingly, however, at both frequencies another EPR signal is detected around $g = 2$ which varies with selenium content. Polyselenide or iron selenide formation could be the origin of these signals. If this proves to be the case it is possible that HFEPR is in fact probing a structure that is key in providing the color and retention in these silicon oxide glasses. The spectrum at 220 GHz contains resolved features that are hardly resolved in the X-band spectra. The comparison of the EPR results with model systems will help to identify and understand the detected centers.

Acknowledgements: This work was supported by NSF grant 5024-54522.

¹ Bassine, J.F., *et al.*, Rivista della Staz. Sper. Vetro, **5**, 95 (1990).

² Mestdagh, M.M., *et al.*, Glass Technology, **24**, 184 (1983).

Far Infrared Magnetoelastic Coupling in Mn_{12} -Acetate

Sushkov, A.B., State Univ. of New York at Binghamton, Chemistry
 Jones, B.R., SUNY-Binghamton, Chemistry
 Musfeldt, J.L., SUNY-Binghamton, Chemistry
 Wang, Y.J., NHMFL
 Achey, R.M., FSU, Chemistry
 Dalal, N.S., FSU, Chemistry

We report the far-infrared spectra of the molecular nanomagnet Mn_{12} -acetate as a function of temperature (4 to 300 K) and magnetic field (0 to 17 T). The large number of vibrational modes is related to the low symmetry of the molecule, and they are grouped together in clusters. Analysis of the mode

character shows that all vibrations are highly mixed and complex. Three features involving intramolecular vibrations of the Mn_{12} -acetate molecular centered at 284, 309, and 409 cm^{-1} show changes with applied field. The structure near 284 cm^{-1} displays the largest deviation with field and is mainly intensity related. Both the absorption difference spectra and the standard deviation from the mean are shown below. Based on the similarity between the temperature and field dependent absorption difference data, we speculate that the 284 cm^{-1} mode may involve $\text{Mn}(3)$ motion in the crown.

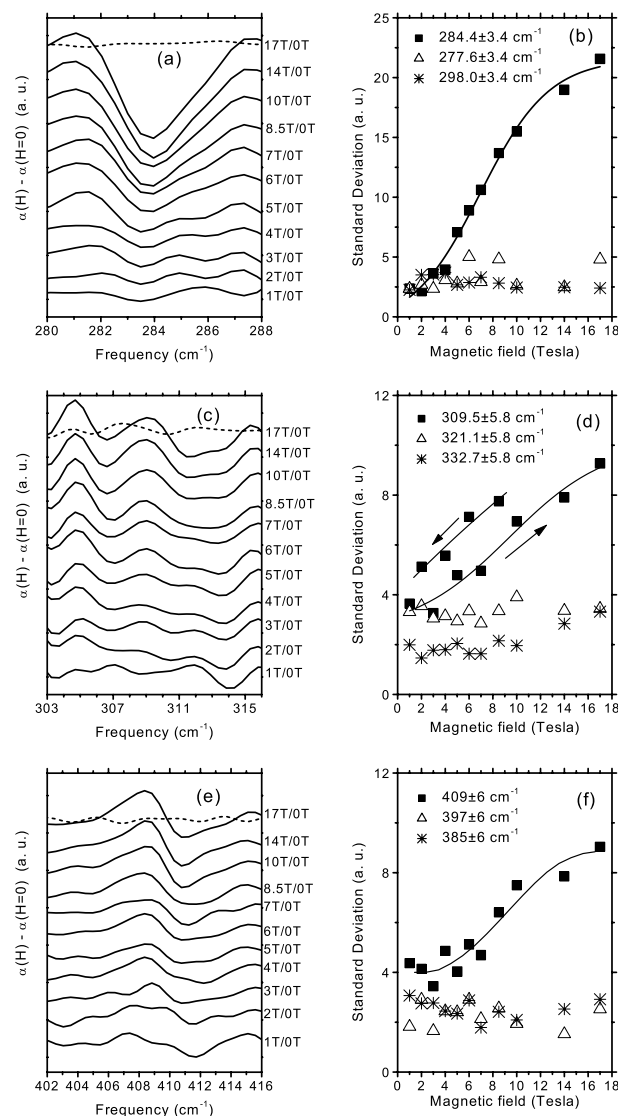


Figure 1. Far infrared absorption difference spectra on Mn_{12} -Ac at different magnetic fields.

Acknowledgements: We are grateful for financial support from the Division of Materials Science at the National Science Foundation (DMR-9623221).

Using Electronic Structure Changes to Map the H-T Phase Diagram of α' - NaV_2O_5

Sushkov, A.B., State Univ. of New York at Binghamton, Chemistry

Musfeldt, J.L., SUNY at Binghamton, Chemistry

Crooker, S.A., LANL/NHMFL

Jeygoudez, J., Universite de Paris-Sud, Laboratoire de Chimie des Solides

Revscolevschi, A., Universite de Paris-Sud, Laboratoire de Chimie des Solides

We have measured the polarized optical reflectance of α' - NaV_2O_5 as a function of temperature (4 to 45 K) and applied magnetic field (0 to 60 T) using the 60 T Long-Pulse magnet. Typical reflectance ratio data is shown below. Rung-directed electronic structure changes as measured by the reflectance ratio $\Delta R(H) = R(H)/R(H=0 \text{ T})$ in the near infrared are especially sensitive to the phase boundaries, and we employ these changes (via analysis of integrated intensities) to map out the H-T phase diagram. Our data is consistent with limited spin Peierls behavior in the vicinity of the triple point. Unexpected strong hysteresis effects in the optical response are observed below 34 K.

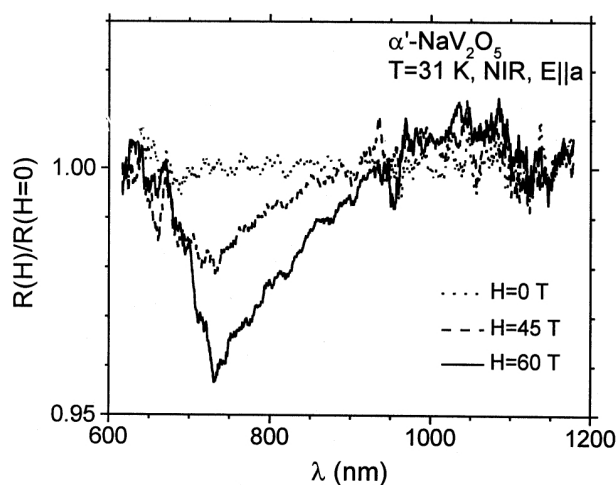


Figure 1. Near infrared reflectance ratio spectra of α' - NaV_2O_5 at 31 K polarized in the rung (a) direction.

Acknowledgements: We are grateful for financial support from the Materials Science Division at the U.S. Department of Energy (DE-FG02-99ER45741).

High Magnetic Field NMR Study of LiVGe_2O_6 , a Quasi 1-D Spin $S=1$ System

Vonlanthen, P., UCLA, Physics and Astronomy

Tanaka, K.B., UCLA, Physics and Astronomy

Clark, W.G., UCLA, Physics and Astronomy

Gavilano, J.L., ETH-Zurich, Switzerland

Ott, H.R., ETH-Zurich, Switzerland

Millet, P., CEMES, France

Mila, F., Univ. of Lausanne, Switzerland, Institute de Physique Theorique

Kuhns, P., NHMFL

Reyes, A.P., NHMFL

Moulton, W.G., NHMFL

Recently, a new quasi 1-D spin $S=1$ system, LiVGe_2O_6 , has been the object of intensive experimental^{1,2,3} and theoretical investigations.⁴ This compound has an antiferromagnetic phase transition at about 25 K and the Haldane gap is either absent or strongly suppressed. Quantum chemistry calculations⁴ indicate a predominant role may be played by a second-order splitting of the t_{2g} orbitals, leading either to significant biquadratic and next-nearest neighbor exchange interactions along the chain, or to an orbital degree of freedom that is involved in the ordering. Although the low temperature phase has a rather simple, long-range antiferromagnetic order,³ several questions about it remain open, including the order of the phase transition and the size and origin of the energy gap in the excitation spectrum.

We have performed ^7Li NMR measurements that include NMR spectra, the spin-lattice relaxation rate ($1/T_1$), and the spin-spin relaxation rate ($1/T_2$) at magnetic fields (B) of 9 T and 23 T and temperatures (T) over the range 1.8 to 300 K. The 9 T measurements were made at UCLA and the 23 T ones used the resistive magnet in Cell 8 at the NHMFL in Tallahassee. The NMR spectra at 9 T show a continuous transfer of spectral weight from a paramagnetic phase to an antiferromagnetic one in a narrow temperature range of about 2 K around the transition temperature $T_N \approx 25$ K. Both phases coexist in this range.

Fig. 1 shows $1/T_1$ as function of T^{-1} in LiVGe_2O_6 at 9 and 23 T. Below 10 K, well into the antiferromagnetic phase, the behavior of $1/T_1$ is consistent with electron spin excitations across an energy gap (Δ) with $\Delta/k_B = 14$ K at 9 T and 11 K at about 23 T; i.e., applying a large B reduces Δ only slightly. Since $g\mu_B B/k_B$ is about 18 K for $B=23$ T, it is surprising that Δ exhibits such a small dependence on B . Furthermore, changing B from 9 to 23 T increases T_N by about 1 K. Thus, T_N is influenced only marginally by B up to 23 T.

Acknowledgements: The UCLA part of the work was supported by NSF Grants DMR-9705369 and DMR-0072524.

¹ Millet, P., *et al.*, Phys. Rev. Lett., **83**, 4176 (1999).

² Gavilano, J.L., *et al.*, Phys. Rev. Lett., **85**, 409 (2000).

³ Lumsden, M.D., *et al.*, Phys. Rev. B, **62**, R9244 (2000).

⁴ Mila, F., *et al.*, Eur. Phys. J.B, **16**, 7 (2000).

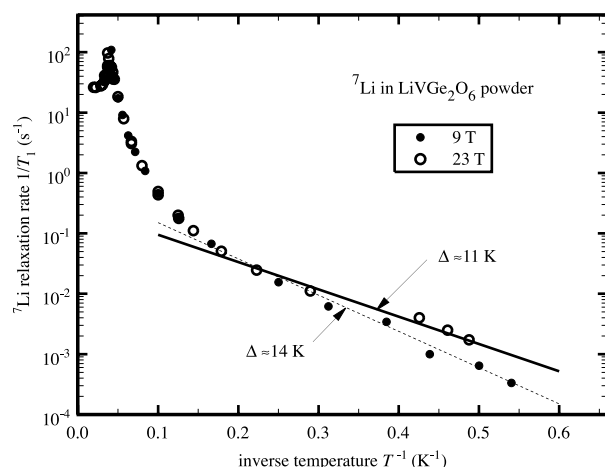


Figure 1. ${}^7\text{Li}$ $1/T_1$ as function of T^{-1} in LiVGe_2O_6 at 9 and 23 T. The solid and the dashed line correspond to gap energies Δ of about 11 and 14 K, respectively.

Characterization of the Novel Low Dimensional Magnetic System $(\text{CH}_3)_2\text{NH}_2\text{CuCl}_3$

Watson, B.C., UF, Physics

Maloney, J.R., UF, Physics

Stock, J.M., Stetson Univ. and UF, Physics

Meisel, M.W., UF, Physics

Hall, D.W., NHMFL

Granroth, G.E., Oak Ridge National Laboratory

Nagler, S.E., Oak Ridge National Laboratory

Jensen, D.A., UF, Chemistry

Backov, R., UF, Chemistry

Petruska, M.A., UF, Chemistry

Fanucci, G.E., UF, Chemistry

Talham, D.R., UF, Chemistry

At room temperature, the crystal structure of the title material was determined to consist of $S = 1/2$ Cu^{2+} spins arranged in isolated zig-zag chains with adjacent chains separated by $(\text{CH}_3)_2\text{NH}_2$ groups.¹ The distance between spins alternates between two values and the bond angle between spins is approximately 90° . Consequently, the magnetic structure is expected to be an antiferromagnetic chain with two alternating exchange constants, J_1 and J_2 . A detailed series of magnetic studies, including magnetization studies in fields up to 30 T at temperatures down to 1.6 K, have provided data that cannot be described by the alternating chain model alone.² A structural transition has been observed near 250 K using EPR, capacitance, and neutron diffraction techniques. In addition, additional features have been observed in the data near 50 K and 11 K. To date, the low temperature crystal structure has not been determined and is the subject of continuing work.

Acknowledgments: This work was supported, in part, by the NSF through the NHMFL REU Program (J.R.M.), the UF Department of Physics REU Program (J.M.S.), DMR-9704225 (B.C.W. and M.W.M.), the NHMFL via DMR-9527035, DMR-9900855 (D.R.T. and co-workers), and by the State of Florida and the UF Center for Condensed Matter Science. Oak Ridge National Laboratory is managed for the DOE by UT-Battelle, LLC, under Contract No. DE-AC05-00OR22725.

¹ Willet, R., J. Chem. Phys., **44**, 39 (1966).

² Watson, B.C., Ph.D. thesis, University of Florida (2000).

The Magnetic Spin Ladder (C₅H₁₂N)₂CuBr₄: High Field Magnetization and Scaling Near Quantum Criticality

Watson, B.C., UF, Physics

Kotov, V.N., UF, Physics

Meisel, M.W., UF, Physics

Hall, D.W., NHMFL

Granroth, G.E., Oak Ridge National Laboratory

Montfrooij, W.T., ORNL

Nagler, S.E., ORNL

Jensen, D.A., UF, Chemistry

Backov, R., UF, Chemistry

Petruska, M.A., UF, Chemistry

Fanucci, G.E., UF, Chemistry

Talham, D.R., UF, Chemistry

Magnetic spin ladders are a class of low dimensional materials with structural and physical properties between those of 1D chains and 2D planes. In a spin ladder, the vertices possess magnetic spins that interact along the legs, via J_{\parallel} , and along the rungs, via J_{\perp} , but are isolated from equivalent sites on adjacent ladders J' , where $J' \ll J_{\parallel}, J_{\perp}$. The magnetization, $M(H \leq 30 \text{ T}, 0.7 \text{ K} \leq T \leq 300 \text{ K})$, from single crystals and powder samples of the title material, has been used to identify this system as an $S=1/2$ Heisenberg two-leg ladder in the strong coupling limit, $J_{\perp}=13.3 \text{ K}$ and $J_{\parallel}=3.8 \text{ K}$, where $H_{c1}=6.6 \text{ T}$ and $H_{c2}=14.6 \text{ T}$.¹ An inflection point in $M(H, T=0.7 \text{ K})$ at half-saturation, $M_s/2$, is described by an effective XXZ chain, as shown in Fig. 1. The data exhibit universal scaling behavior in the vicinity of H_{c1} and H_{c2} , indicating the system is near a quantum critical point.

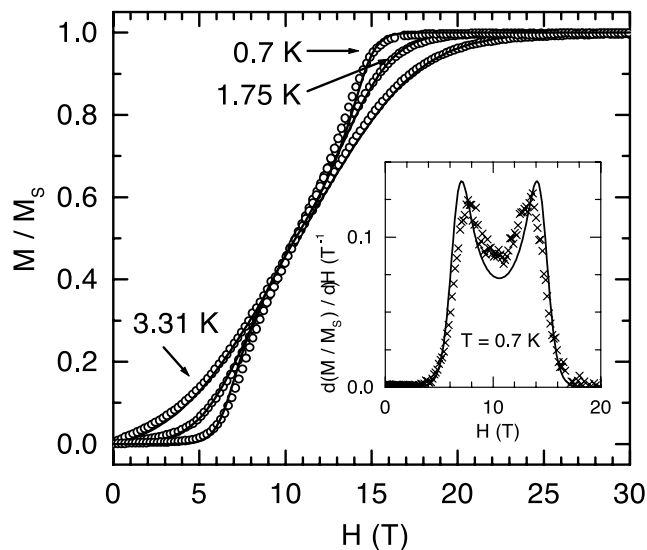


Figure 1. The magnetization, M , of a powder sample (208.2 mg), normalized to its saturation value, is shown as a function of field and temperature. The lines are predictions of an effective XXZ chain when $J_{\perp} = 13.3 \text{ K}$ and $J_{\parallel} = 3.8 \text{ K}$. At 0.7 K , the inflection point at $M_s/2$ is clearly visible, and the inset shows the derivative of this data.

Acknowledgments: This work was supported, in part, by the NSF through DMR-9704225 (B.C.W. and M.W.M.), DMR-9357474 (V.N.K.), the NHMFL via DMR-9527035, DMR-9900855 (D.R.T. and co-workers), and by the State of Florida. Oak Ridge National Laboratory is managed for the DOE by UT-Battelle, LLC, under Contract No. DE-AC05-00OR22725.

¹ Watson, B.C., *et al.*, cond-mat/0011052; and B.C. Watson, Ph.D. thesis, University of Florida (2000).

Thermoelectric Power of Half-Metallic Chromium Dioxide Films

Watts, S.M., FSU, Center for Materials Research
and Technology (MARTECH)

Jaime, M., NHMFL/LANL

von Molnár, S., NHMFL/FSU, MARTECH

CrO₂ is the only known ferromagnetic, metallic binary oxide and is already a technologically important magnetic material in magnetic-recording media. Band calculations¹ predict that CrO₂ is half-metallic: the majority spin has a metallic band structure, while the

minority spin has a semiconductor-like gap. Indeed, films of CrO_2 have shown a record spin polarization of 90% in Andreev reflection measurements at low temperature.² Spin-polarized transport has been a topic of interest since the discovery of giant magnetoresistance (GMR) and has received renewed attention since the re-discovery of colossal magnetoresistance (CMR) in the doped lanthanum manganites.

Watts *et al.*³ have shown recently that the low-temperature, electronic-transport properties in CrO_2 films fabricated by the high-pressure, thermal decomposition of CrO_3 onto (110)-oriented, single-crystal rutile (TiO_2) substrates behave as expected for an almost completely spin-polarized, half-metallic system; i.e., the low-temperature magnetoresistance is positive with a negative component that grows as the temperature increases. The temperature dependence of the resistivity is dominated by a T^2 term that turns itself on exponentially following the functional form $\rho = \rho_0 + AT^2 e^{-\Delta/T}$, where $\Delta = 80$ K. This is characteristic of spin-flip scattering processes and demonstrates the gradual involvement of the down-spin band when temperature is comparable to the energy difference between the fully polarized ground state and a state with a populated down-spin band. Similar physics has been observed in manganites,⁴ where the combined study of electronic and thermal transport provides evidence for energy splinted up-spin and down-spin bands. The only available thermal transport studies for CrO_2 , however, were done in the sixties on compressed powder samples.⁵

We propose to measure the thermoelectric power of CrO_2 textured films in magnetic fields up to 18 T to improve our understanding of the physics in half-metallic systems. The thermoelectric power should in principle be sensitive to the crossover from low-temperature, majority-spin transport to higher-temperature, mixed-spin conduction. The thermoelectric properties in applied magnetic field should help us learn more about the band structure as the band occupation changes with magnetic field and temperature.

To this end, we have successfully prepared the thermoelectric power experiment in the 18 T superconducting magnet system. The experiment is based on a two-heater, quasi-AC (“seesaw”) method,⁶ and has been completely automated with Labview software control and data collection. We have made calibrations with a high- T_c superconductor (superconductors have zero thermoelectric power) from low temperature up to the superconductor’s T_c of ~ 125 K, so that the spurious voltages from the thermocouple leads to the sample can be subtracted. The measurements on CrO_2 completed thus far have indicated complex behavior, such as changes in sign with temperature. In order to understand this behavior and to correlate with electrical transport coefficients, more detailed measurements are planned for both thermopower and regular transport (magnetoresistance and Hall effect) in high magnetic fields.

Acknowledgements: We would like to thank J. Schwartz for providing the high- T_c superconductor. This research is sponsored by DARPA through the Office of Naval Research, ONR Grant No. N00014-99-1-1094.

¹ See, e.g., Schwarz, K., *J. Phys. F: Mat. Phys.*, **16**, L211 (1986); M. A. Korotin, M.A., *et al.*, *Phys. Rev. Lett.*, **80**, 4305 (1998).

² Soulen, R.J., Jr., *et al.*, *Science*, **282**, 85 (1998).

³ Watts, S.M., *et al.*, *Phys. Rev. B*, **61**, 9621 (2000).

⁴ Jaime, M., *et al.*, *Phys. Rev. B*, **58**, R5901 (1999).

⁵ Chapin, D.S., *et al.*, *J. Phys. Chem.*, **69**, 1402 (1965).

⁶ Resel, R., *et al.*, *Rev. Sci. Instrum.*, **67**, 1970 (1996).

Microstructures of LiCu_2O_2 Single Crystal Studied by Transmission Electron Microscopy ▀ IHRP ▴

Xin, Y., NHMFL
Cao, G., NHMFL
Moulton, W.G., NHMFL
Crow, J.E., NHMFL

Mixed-valent LiCu_2O_2 shows interesting magnetic and resonance properties. The knowledge of the crystallographic structure is important in interpreting the observed physical properties. It has been noted that LiCu_2O_2 has an orthorhombic structure,¹ rather than tetragonal one as reported earlier.² In this report, a characterization of the crystal structure and microstructure of the self-flux grown single crystal by transmission electron microscopy (TEM) is presented. The size of typical LiCu_2O_2 single crystals is $3 \times 2 \times 1$ mm. The crystal structure determined

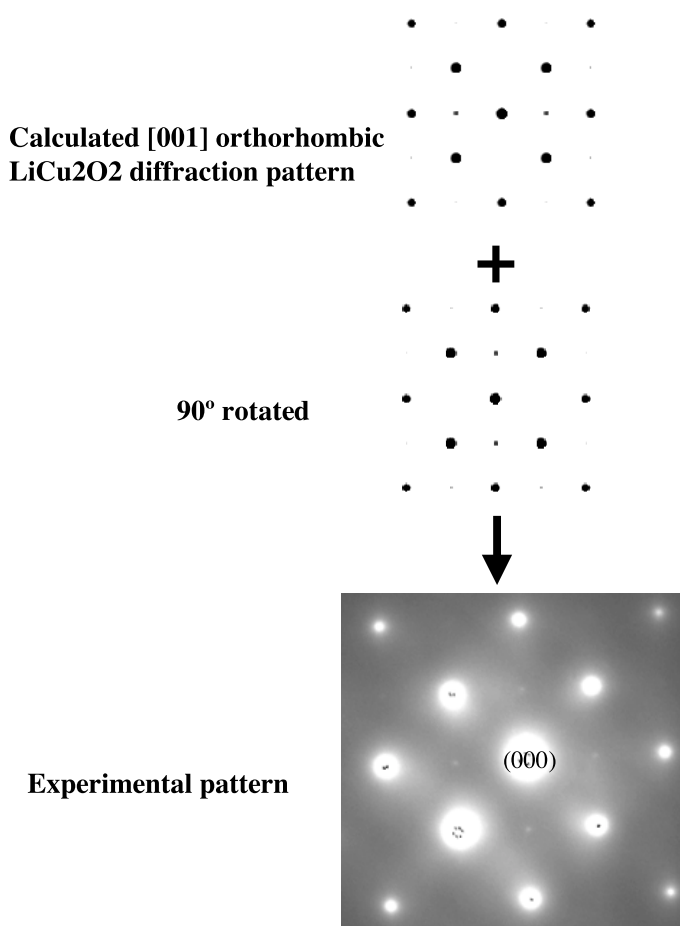


Figure 1. Calculated [001] diffraction pattern of Li_2CuO_2 with orthorhombic structure and the twinned experimental one.

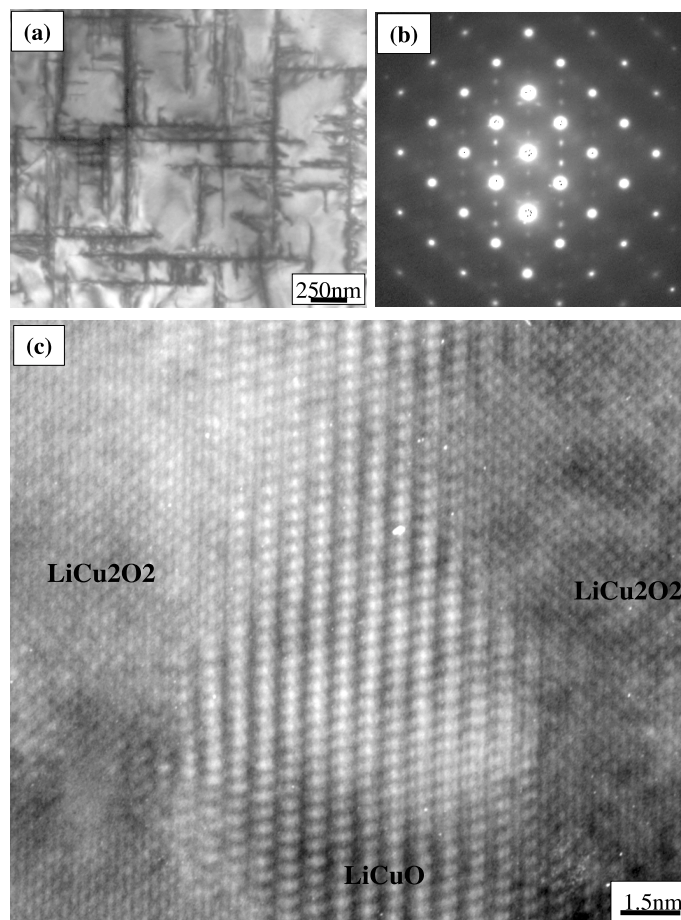


Figure 2. (a) Bright field TEM image showing the second phase precipitates; (b) SAD pattern of $[1-22]_{\text{LiCu}_2\text{O}_2}/[111]_{\text{LiCuO}}$; and (c) HRTEM image of the precipitate.

from nearly perfect regions of the crystal is orthorhombic, but twinned at the microscopic level, as shown in Fig. 1. The weak reflections indicated the orthorhombic structure with twinning. The weak reflections for a tetragonal structure would be in different positions, i.e., between the transmitted spot (000) and the shortest diffraction spots. This confirms that the LiCu_2O_2 indeed has orthorhombic structure.

The bulk material of the crystal is clearly the LiCu_2O_2 phase; however, there is a second phase in the form of platelets with the dimension of about $100 \times 7 \times 100$ nm dispersed almost regularly inside LiCu_2O_2 , which is about 4% to 8% of the total volume percentage. A bright field TEM image is shown in Fig. 2a. The precipitates appear as dark lines which are separated by the smallest distance of about 77 nm. In the Li-Cu-O system,

there are three well characterized phases, LiCuO, Li_2CuO_2 , and LiCu_2O_2 , which could be synthesized by reaction between Li_2O , Cu_2O , and CuO at elevated temperature. It is determined from several zone axis diffraction patterns that the second phase in the crystal is LiCuO. Fig. 2b is a selected area diffraction (SAD) from both the LiCu_2O_2 matrix and LiCuO second phase, down $[1-22]_{\text{LiCu}_2\text{O}_2}/[111]_{\text{LiCuO}}$. Fig. 2c is a high resolution TEM (HRTEM) image of the precipitate looked at edge-on, which shows the roughness of the LiCu_2O_2 matrix/LiCuO precipitate interface on atomic scale, though generally $(210)_{\text{LiCu}_2\text{O}_2}/(1-10)_{\text{LiCuO}}$.

The enthalpy of formation of LiCuO as compared to the other two phases, Li_2CuO_2 , and LiCu_2O_2 , indicated that it is an intermediate, less stable phase.³ Therefore, it is reasonable that these second phase plates are precipitated during the cooling stage of the crystal growth. Further work on eliminating the LiCuO phase by annealing under oxygen is being carried out, which will improve the quality of the crystal, and in turn improve the data quality of the physical property studies.

¹ Berger, B., *et al.*, J. of less-common metals, **175**, 119-129 (1991).

² Hibble, S.J., *et al.*, J. Solid State Chem., **88**, 534 (1990).

³ Patat, S., Solid State Ionics, **46**, 325-329 (1991).

Magnetoresistance Anisotropy in Bismuth Antidot Arrays in High Magnetic Field

Yang, F.Y., Johns Hopkins Univ., Physics and Astronomy

Strijkers, G.J., Johns Hopkins Univ., Physics and Astronomy

Reich, D.H., Johns Hopkins Univ., Physics and Astronomy

Searson, P.C., Johns Hopkins Univ., Materials Science Engineering

Chien, C.L., Johns Hopkins University, Physics and Astronomy

Parker, J.S., FSU, MARTECH

Xiong, P., FSU, MARTECH

Strelniker, Y.M., Tel Aviv Univ., Physics and Astronomy

Bergman, D.J., Tel Aviv Univ., Physics and Astronomy

In the presence of a strong magnetic field, the resistance of a conducting thin film with an array of holes (antidot array) can exhibit a strong angular dependence on the direction of the magnetic field. The effect is the result of the interactions between the rod-shaped regions of strong current distortions around the voids.¹ A first experimental signature of these effects has previously been observed in fields up to 12 T in GaAs.² In this work, we present measurements of the magnetoresistance anisotropy in bismuth antidot arrays. Because of its large $\mu|B|$ value of over 100 and long electron mean free path of up to 20 μm at 5 K, where μ is the carrier mobility and B the applied magnetic field, bismuth is ideally suited to study the predicted anisotropy effects. The periodic antidot array of bismuth has been produced by optical lithography and electrodeposition.^{3,4} A pronounced angular dependence in the high-field magnetoresistance has been observed. The first sample has a hole diameter of 5 μm and spacing of 9 μm between holes, which exhibits interactions up to the next-nearest neighbors in a field up to 15 T. The second sample has a hole diameter of 4 μm and spacing of 16 μm , which shows interactions up to the third nearest neighbors, as shown in Fig. 1. The measurements can be understood and quantitatively reproduced by theoretical calculations.

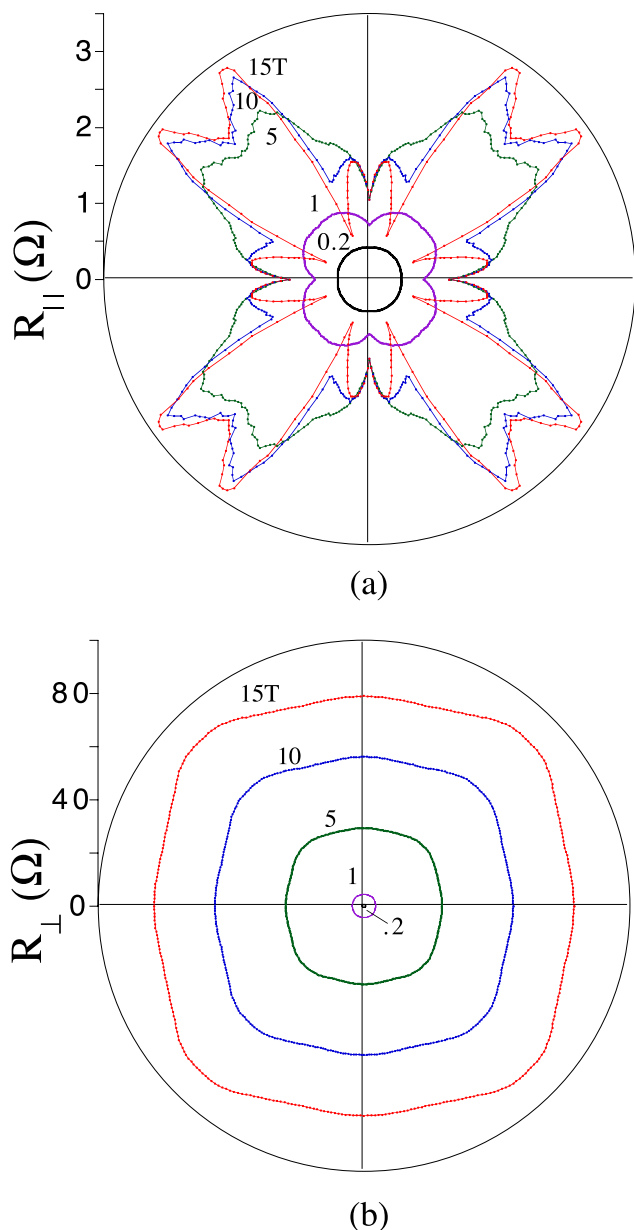


Figure 1. (a) The parallel and (b) perpendicular magneto-resistance of bismuth antidot array with hole diameter of 4 μm and spacing of 16 μm in a magnetic field of 0.2, 1, 5, 10, and 15 T.

Acknowledgements: This work was supported by NSF Grant No. DMR96-80031.

¹ Bergman, D.J., *et al.*, Phys. Rev. B, **49**, 16256 (1994).

² Tornow, M., *et al.*, Phys. Rev. Lett., **77**, 147(1996).

³ Yang, F.Y., *et al.*, Science, **284**, 1335 (1999).

⁴ Yang, F.Y. *et al.*, Phys. Rev. Lett., **82**, 3328 (1999).

Ferromagnetic, A-Type, and Charge-Ordered CE-Type States in Doped Manganites Using Jahn-Teller Phonons

Yunoki, S., NHMFL

Hotta, T., NHMFL

Dagotto, E., NHMFL/FSU, Physics

The two-orbital model for manganites with both non-cooperative and cooperative Jahn-Teller phonons is studied at hole density $x=0.5$ using Monte Carlo techniques.¹ The phase diagram is obtained varying the electron-phonon coupling and the $t(2g)$ -spins exchange. The insulating CE-type charge- and orbital-ordered state with the z-axis charge stacking observed in narrow-bandwidth manganites is stabilized in the simulations. Its charge gap $\Delta(\text{CO})$ is much larger than the critical temperature $k_B T(\text{CO})$. Metallic-like A-type and ferromagnetic states are also obtained in the same framework, and the phase boundaries among them have first-order characteristics.

¹ Yunoki, S., *et al.*, Phys. Rev. Lett., **84**, 3714 (2000)

Electron-Spin Resonance Investigation of the Spin-Chain System LiCu_2O_2

■ IHRP ▲

Zvyagin, S., NHMFL

Cao, G., NHMFL

Brunel, L.-C., NHMFL

Crow, J., NHMFL

The results of the high-frequency electron-spin resonance investigation of the spin-chain system LiCu_2O_2 are presented. We have found that at high temperatures ($T > 23$ K), there is a linear resonance branch that corresponds to a g-factor of 2.29 (BIIc). Temperature dependence of the absorption line intensity demonstrates a pronounced maximum which corresponds to transitions within the exciting states (Fig. 1). The study of LiCu_2O_2 has revealed a spin-singlet ground state, separated from the first excited triplet by a gap $\Delta \sim 67$ K. Our results confirm

a phase transition at $T=23$ K, which manifests itself in the significant broadening of the absorption line. This behavior can be explained in terms of the spin correlation enhancement, as seen also by specific heat and magnetic susceptibility measurements.

Acknowledgements: This work was supported through the NHMFL by NSF DMR 9527035 and the State of Florida.

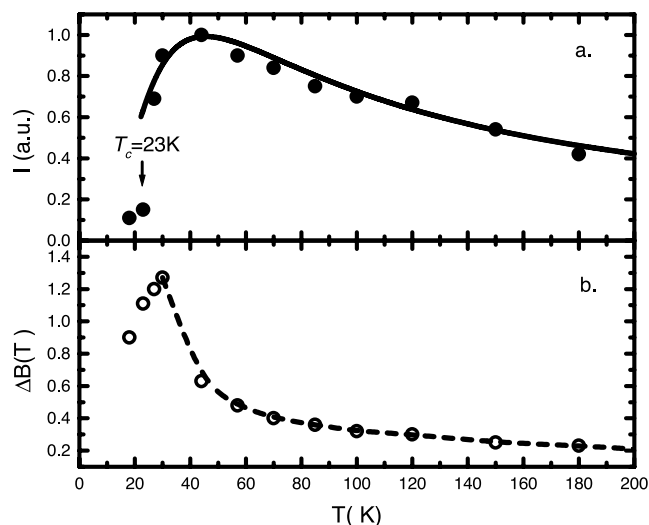


Figure 1. (a) Absorption strength vs. temperature for a resonance line at 277 GHz. The full line is a fit using singlet-triplet model, $\Delta \sim 67$ K. (b) Temperature dependence of the resonance line width (277 GHz). The dashed line is a guide for the eyes.

Microwave Evidences of the Metal-Insulator Phase Transition in Cu(DMe-DCNQI)₂ System with Partial Deuteration

■ IHRP ■

Zvyagin, S., NHMFL
 Angerhofer, A., NHMFL/UF, Chemistry
 Brunel, L.-C., NHMFL
 Von Schütz, J., Univ. of Stuttgart, Physics

High frequency electron-spin resonance investigation of partially deuterated Cu(2,5-dimethyl-N,N'-dicyanoquinonediimine)₂ [Cu(DMe-DCNQI-d₆)₂] (only the methyl groups were deuterated) single-crystals has been performed. We have found that at low temperatures ($T < 78$ K) there is a linear resonance branch that is corresponding to a g -factor of 2.07 ($B \perp c$). A sudden and significant drop in the resonance absorption intensity was observed at the temperature

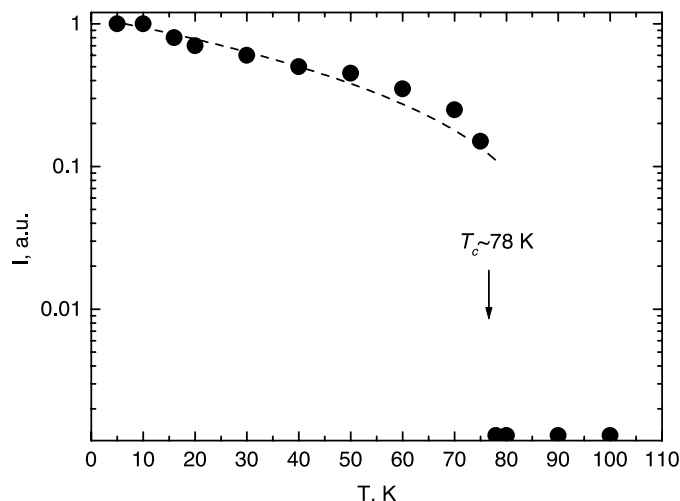


Figure 1. Absorption strength vs. temperature for the resonance line at 287.4 GHz. The dashed line is a guide for the eyes.

of the structural phase transition of about 78 K (Fig. 1). This transition corresponds to a Peierls transition, opening a gap in the metallic conduction band that causes the conductivity of the (high-temperature) metal to drop over eight orders of magnitude. We observe that the insulator-to-metal phase transition in Cu(DMe-DCNQI-d₆)₂ is accompanied by a sudden decrease in the transparency to *mm*- and *sub-mm*-waves. This is one of the characteristic changes that needs to be exploited in order to use this material for high-frequency switches.

Acknowledgements: This work was supported by the NHMFL In-House Grant "Ultrafast Switches for Pulsed Sub-mm Radiation."

Microwave Properties of Nd_{0.5}Sr_{0.5}MnO₃: The Key Role of Orbital Effects

■ IHRP ■

Zvyagin, S., NHMFL
 Kamenev, K., The Univ. of Edinburgh, Physics and Astronomy
 Paul, D.M., Univ. of Warwick, Physics
 Balakrishnan, G., Univ. of Warwick, Physics
 Brunel L.-C., NHMFL
 Angerhofer, A., NHMFL/UF, Chemistry

Bulk properties of the colossal magnetoresistive compound Nd_{0.5}Sr_{0.5}MnO₃ have been studied in the

mm- and *submm*- wavelength spectral range. The relatively high transparency of the material in the metallic ferromagnetic state indicates a significant suppression of the coherent Drude weight. A considerable increase in the microwave transmission has been observed at the transition from an antiferromagnetic to a ferromagnetic phase induced by magnetic field or temperature. Melting of the metallic A-type antiferromagnetic (AFM_A) state has been found responsible for the observed microwave anomaly (Fig. 1), suggesting that the $d(x^2-y^2)$ -orbital degree of freedom plays a significant role in the low-energy optical properties of $\text{Nd}_{0.5}\text{Sr}_{0.5}\text{MnO}_3$. The obtained results provide a strong support for the recent theoretical calculations, based on the orbital-liquid concept.¹

Acknowledgements: This work was supported, in part, by the In-House NHMFL Grant “Ultrafast Switches for Pulsed Sub-mm Radiation.”

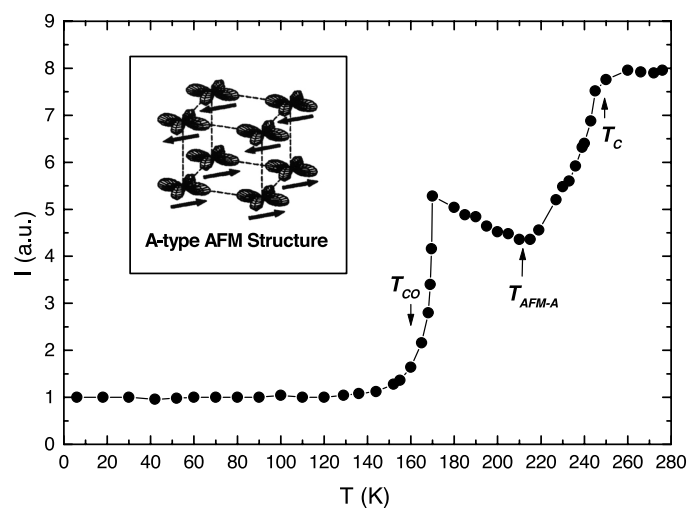


Figure 1. The transmission of $\text{Nd}_{0.5}\text{Sr}_{0.5}\text{MnO}_3$ as a function of temperature at the frequency of 92.6 GHz. The lines are guides for the eyes. The inset shows schematic picture of the ordering of the e_g -orbitals in the AFM_A -type phase.

¹ Ishihara, S., *et al.*, Phys. Rev. B, **56**, 686 (1997).